

# **Analysis and Correlation Study of Human Masseter Muscle with EMG, Ultrasonography & 3D Imaging**



**Shazia Naser-ud-Din**

BDS, MSc (Orthodontics), DPHDent, FICCCDE, DCPSP-HPE

**Thesis submitted for the degree of**

**Doctor of Philosophy**

**The University of Adelaide**

**September 2009**

(This paper has been submitted to the American Journal of Orthodontics and  
Dentofacial Orthopaedics )

## 6 MASSETER LENGTH DETERMINES MUSCLE SPINDLE REFLEX EXCITABILITY DURING JAW CLOSING MOVEMENTS

NASER-UD-DIN S.<sup>a</sup>, SOWMAN P.F.<sup>b</sup>, SAMPSON W.J.<sup>c</sup>, DREYER C.W.<sup>d</sup>,  
TÜRKER K.S.<sup>e</sup>

<sup>a</sup> PhD Candidate Orthodontics (University of Adelaide, Australia), BDS, DPH  
Dent, MSc (Ortho) DCPSP – HPE ,FICCDE Orthodontic Unit, School of  
Dentistry , University of Adelaide, Adelaide, SA, Australia

<sup>b</sup> BPhy, PGDipHSc, PhD, NHMRC Postdoctoral Training Fellow, Macquarie  
Centre for Cognitive Science (MACCS), Macquarie University, Sydney,  
AUSTRALIA

<sup>c</sup> BDS, BSciDent (Hons), MDS, FDSRCS (Eng), FICD, FADI, Begg Chair,  
Orthodontic Unit, School of Dentistry, University of Adelaide, Adelaide , SA, Australia

<sup>d</sup> PhD, MDS, BDS, MRACDS (Orth) FRACDS, FICD, G Cert Ed (HE), Orthodontic  
Unit, School of Dentistry, University of Adelaide , Adelaide, SA, Australia

<sup>e</sup> Centre for Brain Research, Department of Physiology, Faculty of Medicine, Ege  
University, Bornova, Izmir, TURKEY

Reprint requests to:

Professor Kemal S. Türker

Marie Curie Chair of the European Union

Center for Brain Research

Department of Physiology

Ege University Faculty of Medicine

Bornova, Izmir

TURKEY

Mob: + 905394945800

Email: Türker.77@gmail.com

## 6.1 ABSTRACT

### INTRODUCTION

The masticatory muscles are considered to be important determinants of facial form but little is known of the muscle spindle reflex characteristics and their relationship, if any, to face height. The aim of the study was to determine whether spindle reflexes, evoked by orthogonal mechanical stimulation of an incisor tooth and recorded on the masseter muscle, correlated with different facial patterns.

### METHODS

Twenty eight adult volunteers (16 females; age range 19-38years) were subjected to 2 N tap stimuli to their upper left central incisor during simulated mastication. The reflexes were re-recorded with local anaesthesia of the stimulated tooth to eliminate the reflex contribution from periodontal mechanoreceptors (PMR's). Surface electromyograms (SEMG) of the reflex responses of the jaw muscles to these taps were recorded via bipolar electrodes on the masseter muscle and interpreted using spike-triggered averaging of the SEMG. Lateral cephalometric analysis was carried out with Dolphin<sup>®</sup>10.5 and Mona Lisa<sup>®</sup> software.

### RESULTS

2N tooth taps produced principally excitatory reflex responses with a latency of about 17ms post-stimulus. Correlation analysis showed a significant relationship existed between the muscle spindle reflexes and facial heights; specifically, the shorter face height individuals were associated with stronger spindle reflexes. This correlation was strongest between the derived measure of masseter length and spindle reflex strength during jaw closure ( $r = -0.49$ ,  $p = 0.008$ ).

### CONCLUSIONS

These results suggest that a similar muscle spindle stimulus will generate a stronger reflex activation in the jaw muscles of shorter faced individuals compared with the longer faced individuals. This finding may help explain the higher incidence of clenching/bruxism in short-faced individuals and also may in the future influence the design of orthodontic appliances and or dental prosthesis.

## 6.2 INTRODUCTION

Treatment planning is an integral part of orthodontics and is considered incomplete without an assessment of the facial form. Numerous assessments are available<sup>178-185</sup> and some have been closely associated with functional appliance philosophies.

Although substantial work has been done to evaluate the nature of various trigeminal reflexes<sup>1-3</sup> limited research has considered<sup>1-3</sup> the influence facial morphology might have on reflexes from the muscle spindles<sup>4</sup>. This is primarily due to the inherent complexity of studying jaw reflexes during mastication. Most often, the method used to elicit a muscle spindle reflex in the human jaw involves a brief mechanical depression of the mandible, either by use of a tendon hammer or, if a more controlled stimulus is required, a computer-modulated stretching device<sup>5, 6</sup>. An alternative method to the jaw-jerk reflex, the periodontal-masseteric reflex<sup>26, 70</sup>, has been used to assess jaw muscle spindle excitability. In these studies, an upper tooth is tapped and the jaw muscle spindles are excited via vibration transmitted through the upper jaw. Sensitivity of spindles to vibration is well established<sup>186</sup> and hence it is not surprising that vibration applied to a tooth can activate spindles in jaw muscles.

However, this short latency excitatory reflex response has been criticized to have come from a methodological error of the EMG rectification<sup>187</sup>. Nevertheless, recent studies where the stimulated tooth has been locally anaesthetized have shown that the short latency excitatory reflex response actually increased in strength in the absence of the periodontal feedback<sup>70</sup>. These experiments illustrated that the short latency excitatory reflex response in the jaw muscles is a genuine reflex and that it has been normally cut short by the inhibitory reflex response of the simultaneously activated periodontal mechanoreceptors<sup>70, 102</sup>. When the stimulated tooth is locally anaesthetized, the periodontal ligament-induced inhibitory reflex response disappears and the excitatory spindle reflex response becomes completely unveiled.

In the current study, the 'upper incisor tap' method of activating the jaw muscle spindles was used to avoid generating jaw movement which would stimulate other confounding proprioceptors. Local anaesthetic was used to block all neighbouring periodontal mechanoreceptor activity from canine to canine in both upper and lower jaws. These two precautions provided us with the best method of studying jaw muscle spindle reflexes in subjects with different face heights.

To the best of our knowledge no previous work has investigated muscle spindle response and facial height proportions during dynamic masticatory movements. The aim of the current study was to investigate possible correlation between representative facial height measurements and jaw muscle spindle reflex responses from the masseter muscle. Our hypothesis is that muscle spindle reflex responses will not be similar in all face types. The rationale for this proposal is the fact that the length of the spindle and the length of the muscle are positively related<sup>188</sup> and that the same amount of vibration stimulus applied to a muscle will more effectively activate the spindles that are shorter in length. In practise, this would mean that short-face subjects will have a stronger tonus in the jaw muscles compared with the long-faced individuals and may have more likelihood of developing muscle contraction-related problems. If this hypothesis is proven, it may help validate the thickness chosen for plates used to manage bruxism and offer some explanation why orthodontic treatments (primarily functional orthopaedic appliances) vary in their response between individuals.

### **6.3 SUBJECTS AND METHODS**

Experiments were conducted with approval from the University of Adelaide human ethics committee and conformed to the Declaration of Helsinki. A total of 28 volunteers (16 females; age range 19-38 years) were recruited for these experiments. All participants had natural and healthy dentitions, were free of dental symptoms at the time of the experiments and displayed no discernable cranio-facial dysmorphic traits.

#### **6.3.1 EXPERIMENTAL SET-UP**

After taking written informed consent, the subjects were prepared for the experiment. The skin over the left masseter muscle belly was prepared with 70% alcohol swab, to ensure an inter-electrode impedance of less than 5k $\Omega$ . Adhesive EMG electrodes (Duotrode®, Myo Tronics Inc, WA) with 2 cm inter-electrode distance, were affixed to the skin over the left masseter in a superior-inferior configuration.

Grounding of participants was achieved by the use of an ear-clip electrode. Bipolar EMG signals were amplified (1000 – 10000x), filtered (20-1000Hz) and sampled at 2000Hz. EMG recordings presented to participants as online feedback for the static segments of the experiment were full-wave rectified and low-pass filtered (cut-off frequency 1Hz).

Thereafter, each subject was seated comfortably in a dental chair adjusted for height such that the horizontal plane of their upper dental arch was aligned with the horizontal plane of the upper bite plate (Fig.6.1) of the measuring apparatus used in these experiments. This device has been described in detail previously<sup>7</sup>. The bite plates were coated with a semi-rigid dental impression material (3M Express™, Michigan) moulded to each participant's teeth. The upper impression had a small rectangular region cut away to expose the upper left central incisor so it could be contacted on the labial surface and 'tapped upon' by a tooth stimulator.

### 6.3.2 REFLEX RECORDING

Experiments were divided into two main portions, static and dynamic. During static conditions, participants contracted at two different SEMG feedback-controlled isometric levels; "STATIC CLOSING" (corresponding to the EMG evoked during jaw-closing around mid-gape); or "STATIC OPENING" (corresponding to the EMG evoked during jaw-opening around mid-gape). During the isometric contraction the dynamic lower bite bar was set in position-hold mode at the participants' mid-gape jaw position. The stimulus pulse (half sinusoidal 2N pulse with a 10ms rise-time) was superimposed upon a constant tooth preload force of 0.1N. The tooth was stimulated 50 times for each condition (STATIC CLOSING or STATIC OPENING) with a random inter-stimulus interval (3-8 seconds) between stimulus pulses.

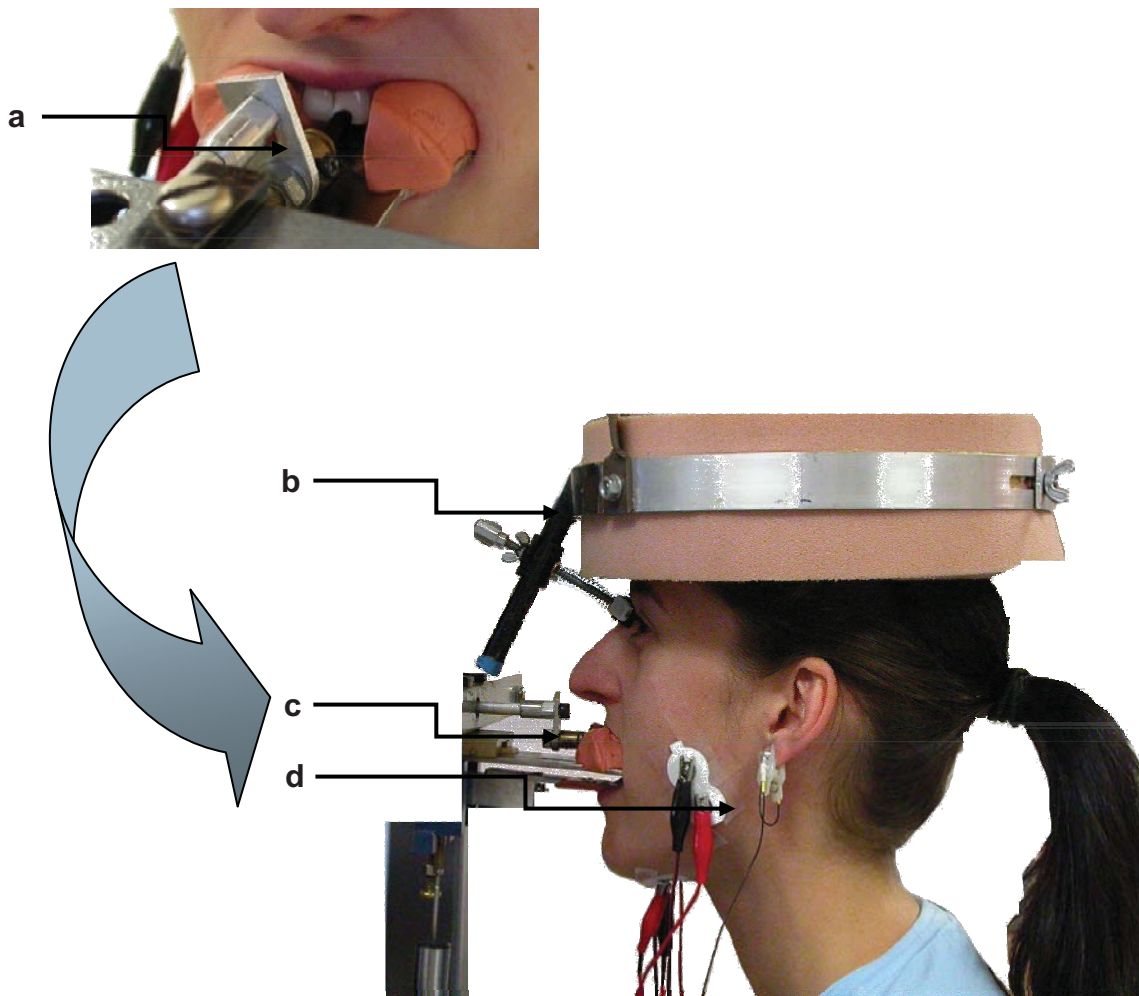


**Fig. 6.1.** Experimental set up with subject positioned on bite plates and orthogonal mechanical stimulation applied onto left central incisor (a). The head halo and nose piece (b) reduces extraneous movements that could contribute to noise in EMG recordings. Custom made impression on bite plates for standardization (c) and transducer delivering pre-determined mechanical stimulation. Surface bipolar electrodes (d) and ear clip for earth.

During the dynamic phase, participants “chewed” against a spring-like resistance provided by a servo-controlled motor. Resistance to jaw closing was inversely proportional to jaw gape, i.e. minimal at maximal opening and maximal (~60N) at occlusion. Participants were instructed to “chew” at a natural pace. Two predetermined stimulus waveforms were output by a dedicated Proportional–Integral–Derivative (PID) loop which controlled the tooth stimulator. These were superimposed upon a constant tooth preload force (0.1N) and consisted either of a half sinusoidal 2N pulse or a pulse of 0N (no stimulus) delivered in response to a trigger that occurred each time the jaw passed through the mid-gape point (~14mm measured inter-incisal). 200 stimuli were delivered during the dynamic trial; 50 2N pulses during closing and opening, and 50 0N pulses during closing and opening.

To ensure a muscle spindle only response was elicited by the tooth stimulation, approximately 4ml of local anaesthetic solution (Xylocaine™, Dentsply) was infiltrated around the incisive papilla, and from canine to canine of both upper and lower jaws in order to block the PMR outflow from the incisor teeth. All reflexes analysed in this study are from stimulus-triggered surface EMG averages obtained during effective local anaesthesia.

### 6.3.3 REFLEX CALCULATION

Rectified EMG was extracted around the trigger time (-50 to +75 ms). The extracted EMGs were sorted with regard to phase of movement (Closing or Opening). In a similar method to that used by Hück *et al.*<sup>83</sup>, EMG with stimulation was normalised by the EMG without stimulation to remove the trend created by the direction of movement. Briefly, the averaged rectified dynamic with stimulus trial was divided point-by-point by its respective no stimulus representation. A 20 ms window starting 15 ms post-stimulus time was constructed and the reflex area (the integral above or below the pre-stimulus mean) was calculated. The strength of the reflex was recorded by expressing it as a percentage of the pre-stimulus area<sup>170</sup> between -5 and -25 ms (Fig.6.2).



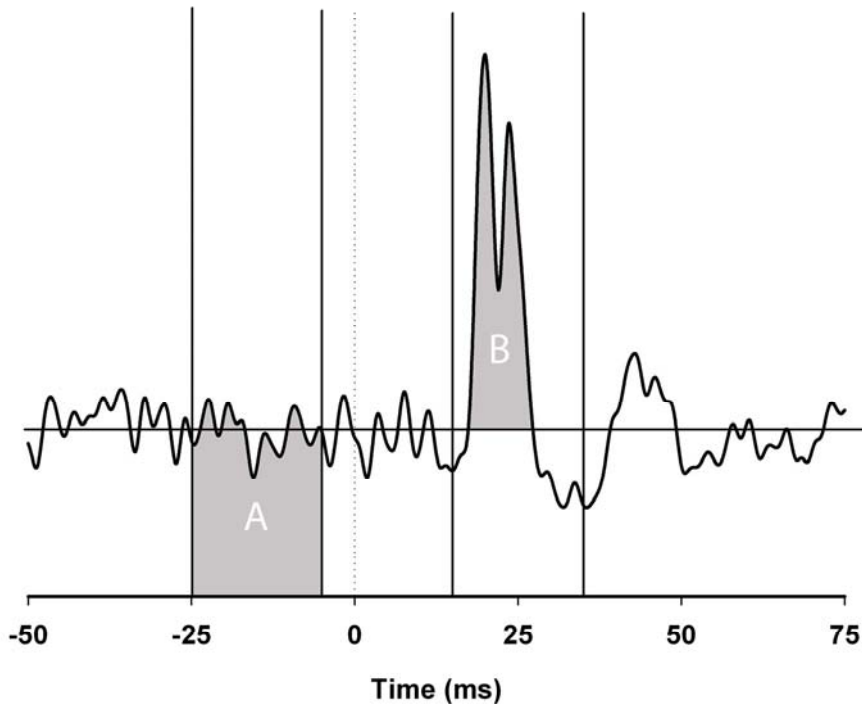


**Fig. 6.2:** Averaged ( $n = 50$ ) muscle spindle mediated reflexes from the left masseter of a single subject. The shaded area B represents the area of excitation. Reflexes were normalised to the level of background excitation by dividing the area B by the area A. Individual reflexes were then correlated to the cephalometric variables for each subject.

#### 6.3.4 CEPHALOMETRICS

Each subject had a standard lateral cephalogram taken with a magnification factor of 1.083 using the Siemens Nador 2 SR system (Bensheim, Germany) with specifications of 220V, 50 Hz and 10amp. The focus-film distance was 150cm and mid-sagittal plane to film distance was 11.5cm. The exposure time was 0.64sec with 75kv and 20mA. Dolphin<sup>®</sup> (Los Angeles, California, USA) and Mona Lisa<sup>®</sup> (Canberra, Australia) cephalometric analysis software systems were used to evaluate linear, angular and proportional facial form variables on scanned lateral cephalograms (Fig.6.3).

### 6.3.5 MASSETER LENGTH

Since the primary aim of this study was to assess the degree of relation between the strength of the masseteric reflex and the length of that muscle as determined by craniofacial morphometry it was appropriate to derive an indirect measure of masseter length (ML) from the lateral cephalogram<sup>31, 120</sup>. For this purpose, cephalometric tracings were performed on standard acetate paper (3M Unitek, Orthodontic Products, Monrovia, CA 91016, USA) with a 0.3mm graphite mechanical pencil in a darkened room. All tracings and digitizations were done by a single investigator (SND). The masseter lengths were measured manually with a digital calliper from zygomatic arch tubercle to gonion.

### 6.3.6 STATISTICAL ANALYSIS

In order to calculate the relationship between the masseteric reflex and those cephalic variables that were most representative of face height, a Factor analysis (FA) with oblique promax rotation was performed and factor scores were calculated for each subject for all variables. Pearson correlation statistics were then calculated to quantify the relationship between ML and the masseteric reflex and subsequently, the relationship between those variables that best represented vertical facial height proportions and the masseteric reflex.

## 6.4 RESULTS

### 6.4.1 MUSCLE SPINDLE RESPONSE DURING MASTICATION

During local anaesthesia of the periodontium surrounding the incisors, mechanical stimulation of the tooth evoked an excitatory reflex response that started ~20ms post-stimulus and terminated ~30ms post-stimulus. An average result for the muscle spindle-only reflex (during local anaesthesia of the stimulated tooth) in one subject with a typical response is shown in Fig.6.2.

### 6.4.2 CEPHALOMETRIC FACTOR ANALYSIS

Factor 1 comprised vertical proportions and specifically ones concentrating in the posterior segment, while Factor 2 was composed of proportional variables. Linear cephalometric Factor 2 correlated significantly with angular cephalometric Factor 1 with  $r = -0.49$  ( $p = 0.008$ ). Similarly angular cephalometric Factor 1 correlated highly with proportional cephalometric Factor 1  $r = 0.65$  ( $p = 0.0002^{**}$ ). There was a significant negative correlation of proportional cephalometric Factor 1 with linear cephalometric Factor 1  $r = -0.62$  ( $p = 0.004$ ). The vertical facial height proportions were best described by masseter length, maxillary-mandibular (Max-Man) plane angle, posterior face height (PFH) and condylion-gonion (Co-Go).

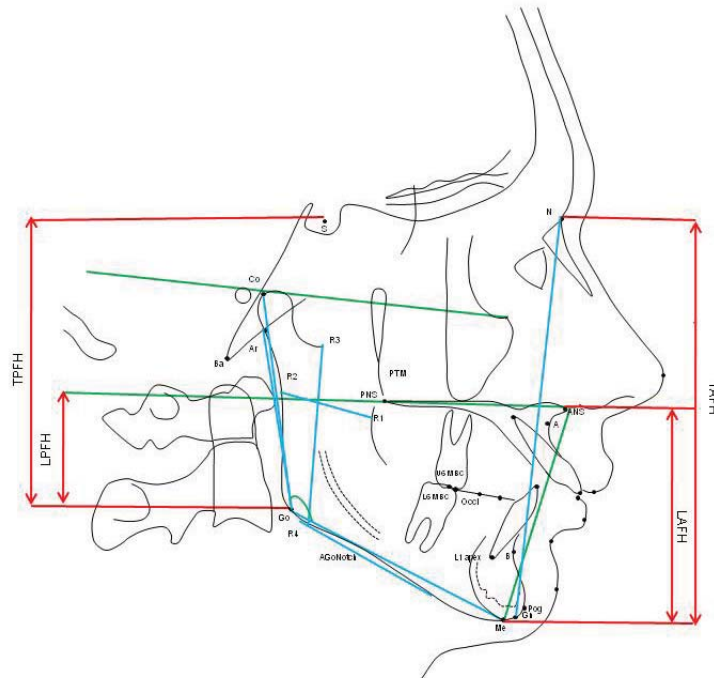


**Fig.6.3:** Lateral Cephalometric analyses with Dolphin<sup>®</sup> 10.5 and Mona Lisa<sup>®</sup> with 9 linear ( Co-Go, Ar-Go, Go-Me, ML, R1-R2, R3-R4, N-Me, N-Gn, AGoNotch), 6 angular ( GoAngle, UGoAngle, LGoAngle, Max-Man, FH-Man, ODI) and 5 proportional (NGn-ArGo, LAFH/TAFH, LPFH/TPFH, ArGo-GoMe, Jarabak Ratio). Colour coordinated to Table 1.

|                        | Variables | Abbreviations                           | Mean       | SD      | Range |             |
|------------------------|-----------|---|------------|---------|-------|-------------|
| Linear Variables       | 1         | Condylion-Gonion                        | Co-Go      | 64.3mm  | (6.0) | 55.4-79.7   |
|                        | 2         | Ante-Gonial Notch                       | Ago-Notch  | 1.9mm   | (0.6) | 0.9-3.2     |
|                        | 3         | Articulare-Gonion                       | Ar-Go      | 45.8mm  | (5.2) | 35.3-55.4   |
|                        | 4         | Gonion-Menton                           | Go-Me      | 73.7mm  | (4.6) | 65.4-80.8   |
|                        | 5         | Nasion-Gnathion                         | N-Gn       | 107.7mm | (6.8) | 96.9-121.3  |
|                        | 6         | Ricketts R1-R2                          | R1-R2      | 29.2mm  | (3.9) | 21.7-36.2   |
|                        | 7         | Ricketts R3-R4                          | R3-R4      | 48.0mm  | (6.5) | 39.6-58.0   |
|                        | 8         | Masseter Length                         | ML         | 56.3mm  | (5.6) | 44.6-65.8   |
|                        | 9         | Nasion-Menton                           | N-Me       | 110.4mm | (7.4) | 99.2-126.6  |
| Angular Variables      | 1         | Maxillary - Mandibular Plane            | Max-Man    | 21.3°   | (6.2) | 10.2-36.5   |
|                        | 2         | Frankfort Horizontal – Mandibular Plane | FH-Man     | 21.8°   | (6.3) | 13.2-36.1   |
|                        | 3         | Upper Gonial Angle                      | Go Angle U | 49.9°   | (5.5) | 41.6-63.6   |
|                        | 4         | Lower Gonial Angle                      | Go Angle L | 68.3°   | (5.2) | 60.1-82.1   |
|                        | 5         | Gonial Angle                            | Go Angle   | 118.2°  | (7.8) | 102.7-134.6 |
|                        | 6         | Overbite Depth Indicator                | ODI        | 73°     | (7.8) | 56.5-92.3   |
| Proportional Variables | 1         | Nasion-Gnathion/ Articulare Gonion      | NGn/ArGo   | 2.2     | (0.2) | 1.8-2.7     |
|                        | 2         | Articulare Gonion / Gonion Menton       | ArGo/GoMe  | 0.7     | (0.1) | 0.6-0.9     |
|                        | 3         | Lower Anterior Face Height              | LAFH/TAFH  | 57.1%   | (3.9) | 47.1-63.3   |
|                        | 4         | Lower Posterior Face Height             | LPFH/TPFH  | 73.4%   | (6.4) | 59.1-84.2   |
|                        | 5         | Jarabak Ratio                           | J Ratio    | 83.6%   | (6.5) | 71.0-95.7   |

**Table 6.1:** Descriptive statistics of 9 linear, 6 angular and 5 proportional cephalometric variables with mean, standard deviations and range.

## Masseter length

For the current study, masseter muscle length was estimated from the bony landmarks of lateral cephalograms with guidelines outlined in previous studies<sup>30, 120</sup>. The spectrum of masseter lengths varied from short through average and long. The range was from 44.6 mm to 65.8mm. The average masseter length was 56.3 mm (+/- 5.57). Two thirds of the sample fell in the average category.

### 6.4.3 CORRELATION BETWEEN MUSCLE SPINDLE REFLEX AND MASSETER MUSCLE LENGTH / VERTICAL FACIAL HEIGHT.

We compared the masseter muscle length and the spindle reflex response and found the following: Under static conditions there was no statistically significant correlation between masseter length and the muscle spindle mediated masseteric reflex. Conversely, when the jaw was closing, a statistically significant relationship ( $r = -0.494$ ,  $p < 0.01$ ) became apparent (Fig.6.4). The shorter the length of the masseter the greater the size of the masseteric excitation evoked by muscle spindle stimulation. This relationship was not apparent during jaw opening. Two of the 3 non-derived cephalometric measures that were shown by factor analysis to best represent face height Co-Go ( $r = -0.417$ ,  $p < 0.05$ ) and Max-Man ( $r = -0.425$ ,  $p < 0.05$ ) were also significantly correlated with the muscle spindle mediated masseteric reflex during jaw closing. PFH ( $r = -0.326$ ,  $p = 0.09$ ) was not significantly correlated with the muscle spindle reflex.

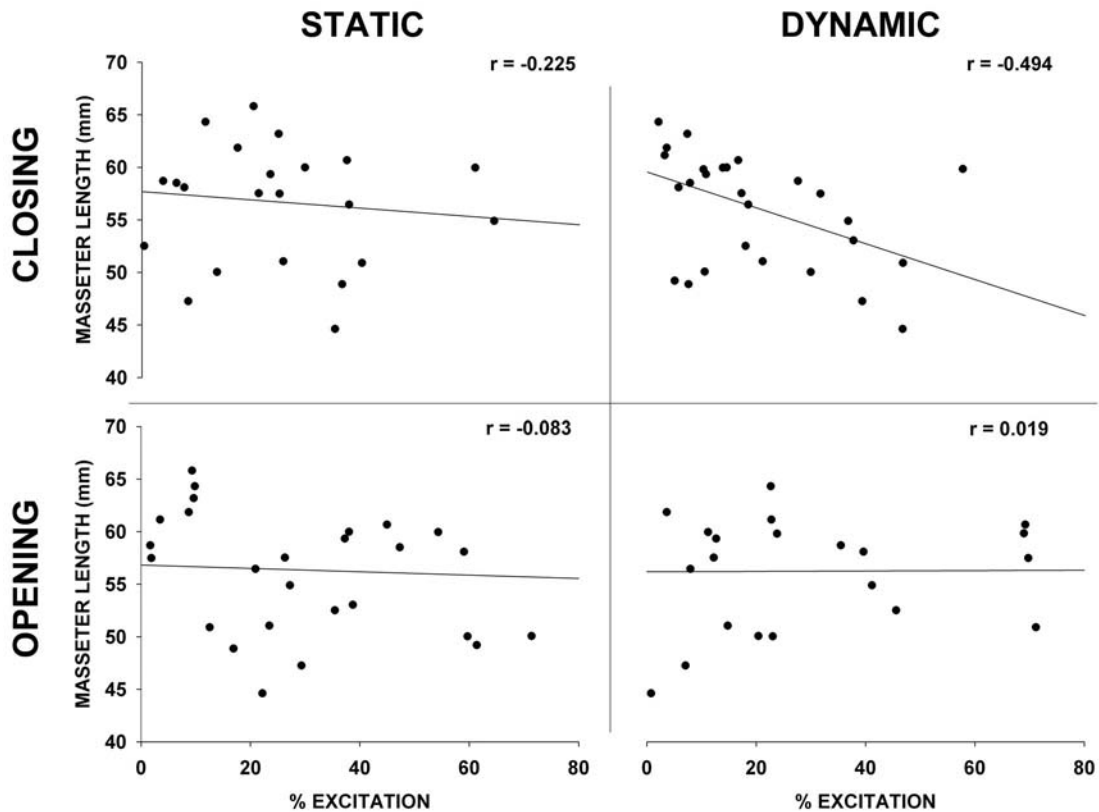


**Fig. 6.4.** Correlations between masseter muscle length and muscle spindle evoked masseteric reflex. Left column illustrates the relationship under static jaw conditions (isometric contractions). Right column illustrates the relationship under dynamic jaw conditions. Reflexes in the top row were recorded either while the jaw was closing or, in the case of the static jaw, with the background EMG matched to the closing EMG. Reflexes in the bottom row were recorded either while the jaw was opening or, in the case of the static jaw, with the background EMG matched to the opening EMG. Pearson  $r$  supplied for each correlation.

## 6.5 DISCUSSION

We found that the masseter muscle length and the vertical face height are significantly related to the size of the muscle spindle reflex response during the jaw closing action. This confirms our hypothesis and suggests that the spindles in the jaw muscles are more sensitive to stimulation during jaw closing in short-faced individuals. It is well known that the gamma efferent activation increases during jaw

closing to compensate for the slackening of spindles and prevent silencing of the spindles<sup>189</sup>. Our findings suggest that the spindles in short-faced subjects (who also have shorter masseter muscles) become more sensitive to further stimulation during jaw closure. This may be due to the more extensive gamma activation in these individuals and/or shorter spindle lengths. Since gamma activation calibrates the spindles to further stimulation, even similar gamma drives may make the short spindles in short muscled individuals more responsive to further stimulation. This is the more likely explanation of our findings.

Muscle spindles in the jaw closing muscles are unique in that they contain the largest number of intrafusal fibres and are thought to contribute greatly to the control of chewing (reviewed in Türker)<sup>3</sup>. By contrast, the jaw openers contain few, if any, muscle spindles. This is quite unique amongst the antagonistic muscle systems in the body. Therefore, the functions of these spindles in the jaw closers are of great interest as they contribute to the tonus in these muscles and may also contribute to development of the bite force<sup>42, 66</sup>. How these receptors function in different face shapes is of interest not only in orthodontic and prosthodontic treatments but also in our understanding of how jaw muscle-related dysfunctions develop in some individuals.

Structured studies<sup>190</sup> and clinical case scenarios<sup>191, 192</sup> have indicated that an important relationship exists between muscle responses, temporo-mandibular disorders (TMD's) and facial patterns. Previous experimental work has demonstrated the significance of facial morphometry in relation to reflex control of jaw muscle tonus. Carels and van Steenberghe showed that successful application of functional orthopaedic appliances is associated with changes in reflex responses of the masseter<sup>193</sup>. The suggestion that underlying neural pathways may contribute to success of the functional treatment needs to be explored. Likewise, protrusive force change was observed with Clark twin blocks<sup>194</sup> again highlighting the interrelationship of muscles and their neurocircuitry. Furthermore, EMG response changes in pre- and post- expansion cases<sup>195</sup> have been demonstrated in the masseter muscle. EMG has been suggested to be useful as a "diagnostic indicator"<sup>196</sup> for TMDs and functional appliance efficiency.

EMG studies have been criticized for not accounting for the natural rhythm of mastication and the overall artificial environment of recording. These two issues were dealt with in an ingenious, but resource intensive study<sup>95</sup>, where portable data recorders and bipolar surface electrodes were used. This study found prolonged muscle activity in adults which in turn was related to the vertical facial types. As might be expected, the short-faced subjects had longer and more sustained masseter muscle activity. In the current study, rhythmic mastication was encouraged in order to simulate natural chewing<sup>30, 40</sup>.

A similar study of EMG and vertical facial factors<sup>96</sup> found negative correlation with muscle efficiency where  $r=-0.39$  ( $p=0.006$ ) which closely relates to the present study where  $r=-0.49$  ( $p=0.008$ )<sup>197</sup> has shown similar findings with mean frequency in closing being  $r=-0.433$  ( $p<0.05$ ) for Ar-Gn and  $r=-0.697$  ( $p<0.001$ ) for N-Me. Strong negative correlations were also found<sup>25</sup> between bite reflexes and face heights<sup>25</sup>. Other interesting findings were with negative correlations in HDC (High Dynamic Close) and PFH where  $r= - 0.34$  ( $p= 0.09$ ) and Co-Go where  $r= -0.42$  ( $p=0.03$ ). Positive correlations with EMG and mandibular plane angles during contractions have also been documented<sup>92</sup> which is similar to our observation of HDC and Max-Man where  $r= 0.43$  ( $p=0.02$ ). The current study, to the best of our knowledge, has looked for the first time into the rhythmic masticatory EMG from masseter muscle spindles as compared to previous work where the morphology and EMG is correlated either in static, relaxed states or with various bite forces<sup>92</sup>.

The plasticity of the masseter muscles and spindles has been well documented<sup>104, 198</sup> and is an area to investigate further in order to enhance the effectiveness of different bite raising appliances. Hence, the present study aimed to find if there was a fundamental difference between the wider spectrum of facial heights and variations in the spindle response. However, the overall sample group had fairly normal vertical proportions according to the ODI which is a predictor of vertical relationships, and its low values indicate a potential open bite. The mean ODI measurement<sup>199</sup> was  $74.5^\circ$  while our sample had a mean of  $73^\circ$  ( $\pm 7.8^\circ$ ) and encompassed no extremes of vertical facial proportion.

Furthermore, since shorter muscles are more likely to develop muscle cramps, it is not surprising that these individuals have more incidences of muscle pain related



problems. It would be interesting to recruit greater extremes of facial disproportion, such as occurs with craniofacial syndromes or major orthognathic surgical cases, to confirm whether masticatory muscle reflexes are different across a wider spectrum of facial types. Furthermore, it would be useful to evaluate muscle dimensions using ultra-sonography, as has been suggested in several studies<sup>128, 130, 200</sup>.

In conclusion, our hypothesis has been supported on the grounds that correlation results showed statistical significance in muscle spindle response among the selected proportions depicting vertical facial heights. Although the study was limited by small sample size and lack of extremes in facial height variation, it does suggest that short- faced individuals have stronger excitatory reflexes especially during jaw closure. This means that they use their spindles much more efficiently compared with the longer-faced individuals and hence may have a higher tonus in their muscle even during rest. This needs to be examined further.

#### 6.5.1 ACKNOWLEDGEMENTS

The authors would like to thank the ADRF (Australian Dental Research Foundation) for financial support. Thanks are also due to Drs Hung Dang and Keng Soon Yeoh (Adelaide Dental Hospital) for their assistance with experiments, to Dr Nancy Briggs (The University of Adelaide) for statistical analyses and Mrs Lucy Hatch for secretarial assistance. KST is supported by the Marie Curie Chair project (Gender Reflex; MEX-CT-2006-040317) and Turkish Scientific and Technological Research Organization (TUBITAK - 107S029 - SBAG-3556). PFS is supported by an NHMRC training fellowship.

(This paper will be submitted to the journal of Investigative Radiology )

## **7 STUDY OF FUNCTION AND FORM FOR HUMAN MASSETER MUSCLE WITH ULTRASONOGRAPHY AND LATERAL CEPHALOMETRICS**

NASER-UD-DIN S.<sup>1</sup> THOIRS K<sup>2</sup>, DREYER C.W.<sup>1</sup>, \*SAMPSON W.J.<sup>1</sup>

1. Orthodontic Unit, School of Dentistry, the University of Adelaide, Adelaide, AUSTRALIA

2. Director Undergraduate Medical Radiation Program & Lecturer in Medical Sonography, City East Campus, University of South Australia, Adelaide, AUSTRALIA

\*Address for correspondence:

Prof WJ Sampson

P.R.Begg Chair in Orthodontics

Orthodontic Unit, School of Dentistry, The University of Adelaide

Adelaide, SA 5000, AUSTRALIA

Tel (08) 8303 3293

Fax (08) 8303 3444

Email: [wayne.sampson@adelaide.edu.au](mailto:wayne.sampson@adelaide.edu.au)

## 7.1 ABSTRACT

Ultrasonography (US) has the potential to be a useful means of investigating the facial musculature. In this study, US was used to correlate the masseter muscle length, thickness and area with corresponding linear, angular and proportional measurements derived from standardized lateral cephalograms. The study aimed to relate US measurements to selected lateral cephalometric variables. An initial pilot study used dried skulls fitted with chicken fillets to simulate the masseter and standardize the methodology. US measurements and direct measurements between bony landmarks representing the masseter length showed a high level of agreement according to Bland and Altman analysis. Standardized lateral cephalometric analysis and US scanning of the left masseter muscle was performed on 11 consenting adults (8 females; age range 22-30 years). 20 cephalometric variables were analysed against three US measurements of the left masseter muscle; length, width and, area and calculated volume. Spearman's rank order correlations were highly statistically significant for area and ramus height (Ar-Go) with  $r = 0.85$  ( $p < 0.001$ ). Overall, repeatability for thickness of the masseter muscle was good (Dahlberg 1.17). Predictive equations from regression analyses were constructed to deduce ramus length from the US measurements, thus potentially obviating repeated cephalometry and associated radiation dose in growing individuals. Our results support the utility of US as a clinical diagnostic tool especially for sequential evaluation of muscle length due to its safety and cost effectiveness. Moreover, it would be a valuable research tool for future facial and muscle growth studies.

### Key words

Ultrasonography, lateral cephalometrics, correlations, human masseter muscle, predictive equations

## 7.2 INTRODUCTION

Over the years, ultrasonography (US) has developed as a valuable static to real time diagnostic medical imaging tool<sup>122</sup> incorporating recent advances in colour mapping and real time 3D imaging<sup>201</sup>. These innovations attempt to improve the image resolution along with better visualization and patient education and communication. US is ubiquitous for its wide application in prenatal imaging due to its safety.

In dentistry, US has established itself as a safe, non-invasive, comfortable and cost-effective adjunct to diagnosis and can produce high resolution images more easily than MRI and CT scans<sup>8</sup>. Future applications of the new resolution imaging capabilities include “*virtual biopsies*” with the acoustic scanning microscope<sup>202</sup>. Another application of US is to evaluate peri-implant health due to better imaging of soft tissues without image distortion from the metal implant. A promising use for US in orthodontics could be to supplement radiographic diagnosis of facial patterns<sup>8</sup>, particularly integument thickness and muscle form, when repeated radiation dose is of concern in children and adolescents.

### 7.2.1 US AND MUSCLES OF MASTICATION

The form and function of the masseter muscle has been investigated using US<sup>23, 27</sup>. A recent comprehensive meta-analysis highlighted the importance of US in the investigation of muscles of mastication as a reliable and convenient method for investigation compared with CT scans and MRI<sup>122</sup>. US has been used to measure differences in masseter muscle thickness in dental arch cross bite cases due to asymmetric muscle activity<sup>23</sup>.

In a pioneer study<sup>17</sup> demonstrated the importance of US for masseter muscle evaluation in adults and its future utility when combined with EMG. In addition, significant correlations between masseter muscle cross-sectional area and linear measurements were demonstrated. Predictive values were recommended in order to

---

deduce additional parameters that would reduce the need to perform cephalometry, which carries risks associated with radiation exposure.

## 7.2.2 US AND FACIAL DIMENSIONS

Investigations have been made into relationships between cephalometric values (linear, angular and proportional variables) and US measurements of masseter muscle dimensions<sup>200, 203</sup>. Mostly, masseter muscle thickness<sup>122</sup> and its relationship to facial morphology has been studied. Relationships between selected cephalometric values and masseter muscle volume<sup>200</sup> and relationships between vertical facial morphology (posterior and anterior facial heights) and masseter muscle thickness<sup>203</sup> have been demonstrated. Most of the research studies have used 3D US for assessment which would neither be cost-effective nor practical in a dental clinical setup for the assessment of masseter muscle. Thus, there is need to use more simple and mobile US systems that can be translated into clinical scenarios.

The aim of the current study was to utilize a simple, cost-effective conventional US method to measure left masseter muscle length, width, and area, and seek correlation with facial proportions selected from the work of Charalampidou *et al.*<sup>203</sup>.

## 7.3 SUBJECTS & METHODS

### 7.3.1 PILOT STUDY

An ultrasound technique called extended field of view (EFOV) was chosen because it provided high resolution images with a high frequency linear array transducer in a field of view large enough to demonstrate the complete length of the masseter muscle in one image. Since EFOV was used for the first time to measure the masseter muscle study it was important to check its accuracy and reproducibility in this setting. In order to validate US measurements, raw chicken meat was used to simulate the masseter muscle on 12 dried human skulls. For each skull, lead markers (7x7mm) were placed on the zygomatic tubercle and gonial angle (Fig 7.1A). The

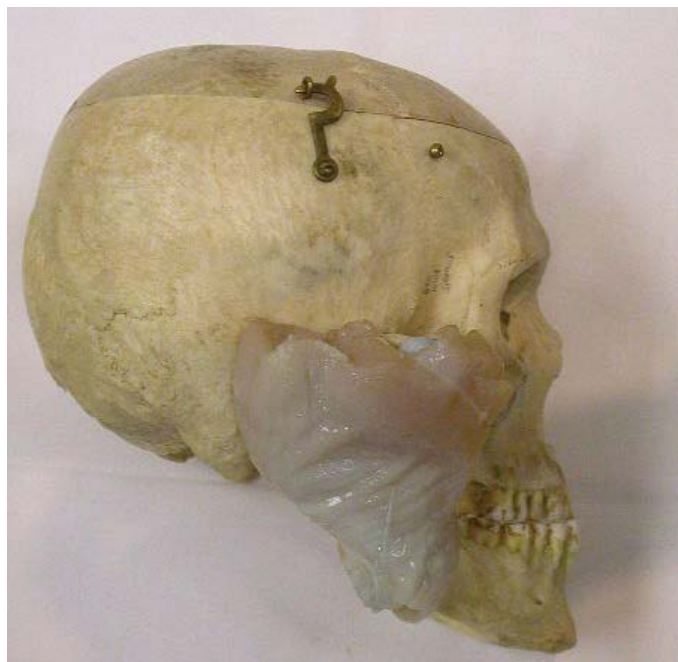
---

mandibular condyles were seated and stabilized in their fossae with Blu Tack (Bostik Australia Pty.Ltd., Victoria, Australia) . The distance between the zygomatic tubercle and the gonial angle was measured using an electronic caliper to represent the length of the masseter muscle with the teeth in occlusion. Chicken meat was then carefully placed over the ramus of the mandible to simulate the soft tissue of the masseter muscle (Fig 7.1B). An experienced, accredited sonographer (KT) produced an EFOV “extended field of view” US image which extended through a plane between the two landmarks identified by the lead markers demonstrating the mandible and the overlaid chicken muscle tissues. The image was produced using a Siemens Antares Sonoline ultrasound machine (Siemens Medical Solutions, USA Inc, Ultrasound Group, Issaquah WA) at the University of South Australia. A 5-13 MHz linear array transducer was used to obtain the image with probe orientation perpendicular to the mandible when acquiring the image. Siescape<sup>®</sup> technology (Siemens Medical Solutions, USA Inc, Ultrasound Group, Issaquah WA) was used to produce an EFOV image, beyond the length of the face of the ultrasound probe. Inherent electronic calipers on the ultrasound machine were then used to measure the distance between the zygomatic tubercle and the gonial angle from the acquired image using the lead markers as a guide.

Acquisition of the ultrasound image and the measurement process was then immediately repeated for each skull. The sonographer was blinded to all measurements throughout the process. A Bland and Altman analysis was used to test the degree of agreement between the first measurements made from ultrasound images and the direct measurements made using electronic calipers (validity), and also between the two measurements made from the ultrasound images for each skull (repeatability).



(A)



(B)

**Fig. 7.1.** Human skulls with lead markers affixed to the zygomatic tubercle and gonial angle with Blu Tack (A) and with chicken fillet simulating the masseter muscle applied with gel for US (B).

### 7.3.2 SUBJECTS

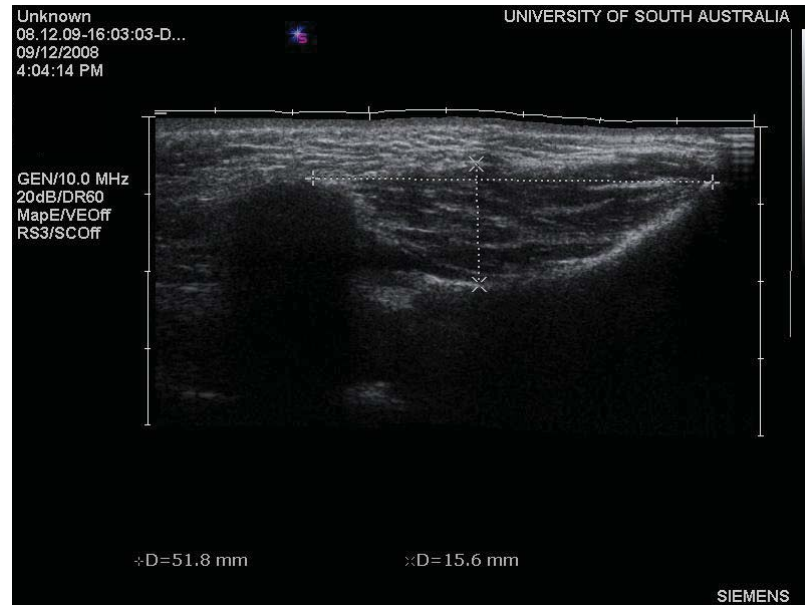
Eleven volunteers (8 females; age range 22-30 years) were recruited to the study. Each subject was provided with a detailed information sheet and written consent was obtained. The study was approved by the Human Ethics committees of The University of Adelaide and University of South Australia independently and according to the Helsinki declaration.

All participants had natural and healthy dentitions, were free of dental and neuro-muscular symptoms at the time of the experiments and displayed no discernable cranio-facial dysmorphic traits.

Unilateral measurements were taken from the left side of each subject for consistency with previous work<sup>204</sup>. 10 weeks later five of the subjects had a repeat measurement.

All scans were conducted in a semi-darkened room. Each subject was comfortably seated with the left side of the face towards the examining sonographer (KT) who explained the procedure. Excessive pressure by the transducer and any resultant soft tissue deformation was reduced by applying generous amounts of gel to the transducer and using light hand-held pressure. Images were obtained in a plane between the zygomatic tubercle to the gonial angle using the same equipment and in the same fashion as the scanning technique in the pilot study. Three images, produced in identical fashion were stored whilst the subject was at maximum clenching intercuspal position with a duration lasting between 10-15sec. After the image was acquired, the sonographer made three measurements from each image using the inherent electronic calipers of the machine; length, thickness and cross-sectional area (Fig 7.2 A). Length of the masseter muscle was measured as the distance between the zygomatic tubercle and the gonial angle. The thickness was measured as the maximum distance between the superficial and deep aspects of the masseter muscle.





(A)



(B)

**Fig. 7.2.** US Scan of the left masseter showing (dotted lines) the length (horizontal line) and the thickness (vertical line) (A). Area was measured manually by tracing the circumference of the masseter muscle (B).

---

Cross-sectional area was measured using a trace tool on the machine which allowed the sonographer to manually trace around the boundaries of the muscle (Fig. 7.2B). Volume of the masseter muscle was calculated for each subject with the height and length measurements provided through the scan with the mathematical deduction for cone volume on the premise it would be an acceptable shape. The formula used was:

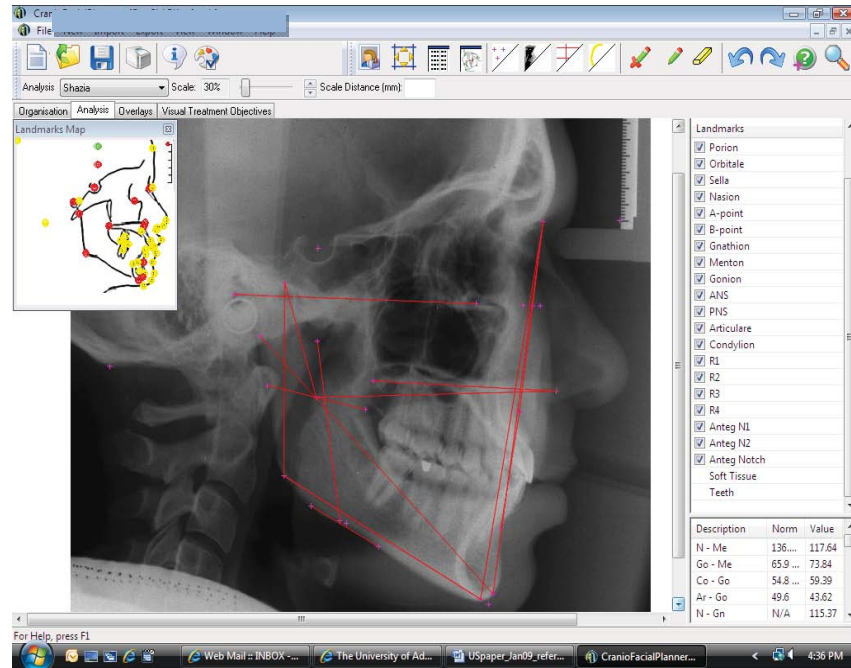
$V = 1/3\pi r.h$ , where V is cone volume, r is radius and h is height.

US (EFOV) facilitated the acquisition of one image from which all measurements were made. EFOV was chosen because the field of view of the high frequency linear array transducer did not cover the entire length of the masseter muscle due to the limited size of the transducer face. EFOV allows an image to be generated beyond the size of the transducer<sup>166</sup>. Our study is the first to report the potential use of EFOV in masseter muscle assessment relevant to orthodontic diagnosis.

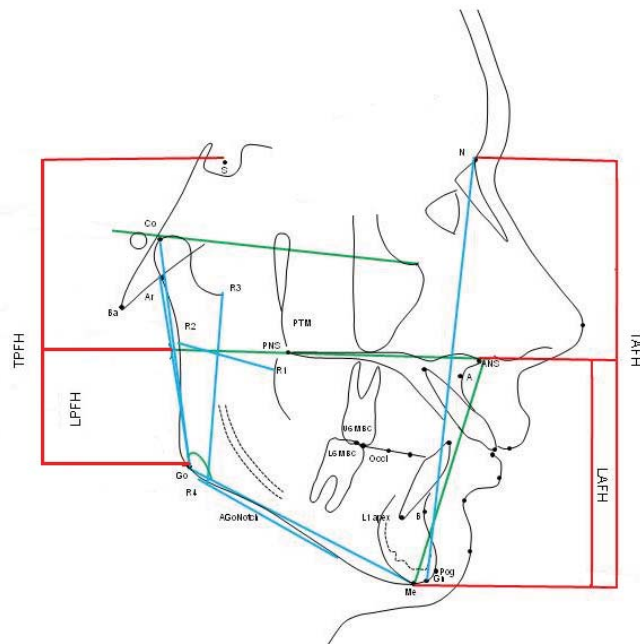
### **Lateral Cephalograms**

Each subject had a standard lateral cephalogram taken with a magnification factor of 1.083 with the Siemens Nador 2 SR system (Bensheim, Germany) with specifications of 220V, 50 Hz and 10amp. The focus-film distance was 150cm and mid-sagittal plane- film distance was 11.5cm. The exposure time was 0.64sec with 75kv and 20mA. Dolphin® (Los Angeles, California, USA) and Mona Lisa® (Tidbinbilla, Canberra, Australia) (Fig. 7.3A) cephalometric analysis software systems were used to evaluate linear, angular and proportional facial skeletal variables from scanned images of the lateral cephalograms.

Cephalometric tracings were performed on standard acetate paper (3M Unitek, Orthodontic Products, Monrovia, CA 91016, USA) with a 0.3mm graphite mechanical pencil in a darkened room for masseter muscle length evaluation only. All tracings and digitization were done by a single investigator (SND).



(A)



(B)

**Fig.7.3.** (A) Lateral Cephalometric measurements made with Mona Lisa® for selected variables i.e Go-Co, Ar-Go, N-Gn, R1-R2, R3-R4, ODI and Ante-Gonial Notch Depth. (B) 9 linear ( Co-Go, Ar-Go, Go-Me, Masseter Length, R1-R2, R3-R4, N-Me, N-Gn, AGoNotch), 6 angular ( GoAngle, UGoAngle, LGoAngle, Max-Man, Frankfort Horizontal to Mandibular plane, ODI) and 5 proportional (NGn-ArGo, LAFH/TAFH,LPFH/TPFH, ArGo-GoMe, Jarabak Ratio).

### 7.3.3 LINEAR CEPHALOMETRIC INDICES

A number of indices have been developed for lateral cephalometrics to provide useful information regarding the vertical and sagittal relationships of the skeletal bases. For this study due to particular interest in the vertical dimension, indices were selected accordingly.

Nine linear indices were selected: (1) condylion-gonion (Co-Go) which indirectly represents the superficial masseter muscle length and ramal length, (2) articulare-Gonion (Ar-Go) giving the mandibular length, (3) nasion-menton (N-Me) gives the anterior face height, (4) gonion-menton (Go-Me) assesses the mandibular body length, and (5) nasion-gnathion (N-Gn) indicates anterior vertical face height<sup>197</sup> (6)R1-R2 and (7) R3-R4 represent the ramus shape<sup>205</sup> and (8) ante-gonial notch (AGoNotch) which is an indicator of mandibular growth rotation and also relates to the facial vertical dimension (9) masseter length from the zygomatic tubercle to gonion angle represent attachment points for superficial masseter muscle. The masseter lengths were measured manually with a digital caliper (Fig 7.3B).

### 7.3.4 ANGULAR CEPHALOMETRIC INDICES

Six angular variables were selected: (1) gonial (Go angle), (2) upper gonial angle (UGo angle), (3) lower gonial angle (LGo angle), (4) Overbite Depth Indicator (ODI)<sup>199</sup>, (5) maxillo-mandibular planes angle and (6) Frankfort Horizontal-Mandibular plane angle (Fig 7.3B).

### 7.3.5 PROPORTIONAL INDICES

Five proportional vertical relationships (1) nasion-gnathion divided by articulare-gonion (NGn/ArGo), (2) Anterior Face Height (LAFH/TAFH) and (3) Posterior Face Height (LPFH/TPFH) which reflect the anterior and posterior vertical proportions, (4) articulare-gonion by gonion-menton (ArGo/GoMe), and (5) Jarabak Ratio (Na-Me/GoAr) (Fig 7.3B).

## 7.4 RESULTS

Descriptive statistics (Table 7.1) provide an overview of cephalometric and US variables. Spearman's rank order correlations between US and cephalometric measurements were utilized due to the small sample size and skewness of the data. 24 variables; 20 cephalometric and four US were analysed (Table 7.1). Correlations were considered moderate at 0.5 while high correlations were at 0.8. The strongest correlations were between the US area measurements and linear and proportional cephalometric measurements. .

Masseter US area had high correlations with two linear indices; Co-Go ( $r=0.81$ ,  $p < 0.002$ ), and with Ar-Go ( $r=0.85$ ,  $p < 0.001$ ). Masseter thickness demonstrated high correlation with R1-R2 ( $r=0.83$ ,  $p < 0.002$ ).

Masseter US area was highly correlated to proportional variables NGn-ArGo ( $r=-0.85$ ,  $p < 0.001$ ) and ArGo-GoMe ( $r= 0.84$ ,  $p < 0.001$ ). Correlations between the cephalometric variables were high for Co-Go with Ar-Gn ( $r=0.80$ ,  $p < 0.01$ ) and Co-Go with R3-R4 ( $r=0.80$ ,  $p < 0.003$ ).

Other lateral cephalometric variables and US measurements with significant correlations are shown in Table 7.2.

### 7.4.1 BLAND AND ALTMAN FOR PILOT STUDY

Bland and Altman plots<sup>167</sup> were used to visually assess and compare the level of agreement between observations. The mean difference is the measure of bias while the variation between the observations fell within the standard deviations. The observation from the pilot study showed (Fig. 7.4) very good agreement.

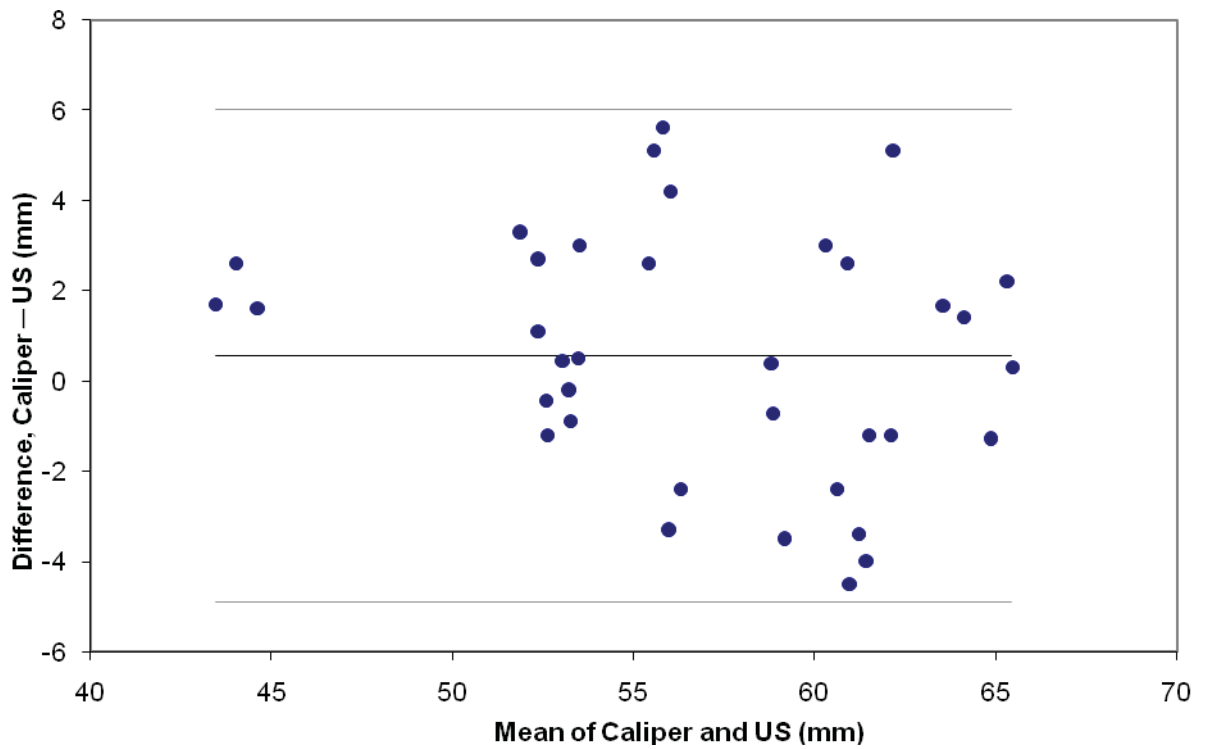


**Fig. 7.4.** Bland and Altman<sup>167</sup> plot depicting extent of agreement for masseter muscle length between the ultrasonography (US) and caliper measurements in the pilot study.

|                                      |   | <b>Variables</b>                               | <b>Abbreviations</b> | <b>Mean</b>            | <b>SD</b> |
|--------------------------------------|---|--|----------------------|------------------------|-----------|
| Linear Cephalometric Variables       | 1 | Condylion – Gonion                             | Co-Go                | 62.2 mm                | 7.2       |
|                                      | 2 | Ante-Gonial Notch                              | AGoNotch             | 1.6 mm                 | 0.6       |
|                                      | 3 | Articulare-Gonion                              | Ar-Go                | 44.2 mm                | 6.2       |
|                                      | 4 | Nasion-Menton                                  | N-Me                 | 108.4 mm               | 5.0       |
|                                      | 5 | Gonion-Menton                                  | Go-Me                | 73.5 mm                | 4.2       |
|                                      | 6 | Nasion-Gnathion                                | N-Gn                 | 106.4 mm               | 5.2       |
|                                      | 7 | Ricketts R1-R2                                 | R1-R2                | 29.1 mm                | 4.3       |
|                                      | 8 | Ricketts R3-R4                                 | R3-R4                | 48.0 mm                | 6.5       |
|                                      | 9 | Masseter Length                                | ML                   | 56.2 mm                | 6.0       |
| Angular Cephalometric Variables      | 1 | Maxillary-Mandibular Plane Angle               | Max-Man              | 21.9°                  | 4.4       |
|                                      | 2 | Frankfort Horizontal to Mandibular Plane Angle | FH-Man               | 23.4°                  | 6.0       |
|                                      | 3 | Overbite Depth Indicator                       | ODI                  | 71.3°                  | 7.8       |
|                                      | 4 | Upper Gonial Angle                             | GoAngleU             | 50.7°                  | 5.4       |
|                                      | 5 | Lower Gonial Angle                             | GoAngleL             | 68.2°                  | 3.2       |
|                                      | 6 | Gonial Angle                                   | GoAngle              | 119.0°                 | 7.2       |
| Proportional Cephalometric Variables | 1 | Nasion-Gnathion / Articulare Gonion            | NGn / ArGo           | 2.3                    | 0.3       |
|                                      | 2 | Articulare Gonion / Gonion Menton              | ArGo / GoMe          | 0.7                    | 0.1       |
|                                      | 3 | Anterior Face Height                           | LAFH/TAFH            | 58.5                   | 2.9       |
|                                      | 4 | Posterior Face Height                          | LPFH/TPFH            | 73.2                   | 7.4       |
|                                      | 5 | Jarabak Ratio                                  | J Ratio              | 83.0                   | 6.5       |
| US Variables                         | 1 | Length   | l                    | 64.7 mm                | 6.8       |
|                                      | 2 | Thickness                                      | t                    | 13.7 mm                | 2.2       |
|                                      | 3 | Area   | a                    | 6.2 mm <sup>2</sup>    | 1.7       |
|                                      | 4 | Volume   | v                    | 3189.0 mm <sup>3</sup> | 973.4     |

**Table 7.1.** Descriptive statistics with cephalometric and US variables of mean and standard deviations.

## 7.4.2 PREDICTIVE EQUATIONS

Pearson correlations show the degree of linear association between two variables and are represented with  $r^{206}$ . Since many studies use this statistical test it is feasible to make comparisons. However, one needs to be mindful of its restrictions; particularly, if there are outliers where the correlation would be strengthened by eliminating them. Therefore, careful scrutiny of descriptive statistics with the range, SD, mean and the p value is important when assessing possible relationships.

Potential predictive variables to estimate cephalometric indices were chosen on the strength of the relationships between US variables and cephalometric variables. Pearson correlations were used to generate simple correlations and linear regressions were used to generate predictive equations. Predictive equations are considered plausible when there is high correlation, statistical significance and a simple formula format. Hence, variables with statistically significant correlations (p-value  $\leq 0.05$ ) were included for generating predictive equations. Predictive equations are presented in Table 7.3 with the correlations and mean standard error.

## 7.4.1 REPRODUCIBILITY

The Dahlberg statistic was used to assess the reproducibility between the US scans which were performed on five subjects 10 weeks after the first measurement. The Dahlberg statistic was 1.3 (good reproducibility) for length measurements and 1.17 (good reproducibility) for thickness.



| VARIABLES                       |  | Correlations &<br>P Values |
|---------------------------------|--|----------------------------|
| Masseter Muscle Length ( US)    | Frankfort Horizontal –Mandibular Plane ( LC) | r = -0.58<br>P = 0.06      |
| Masseter Muscle Area ( US)      | Frankfort Horizontal –Mandibular Plane ( LC) | r = -0.54<br>P = 0.08      |
| Masseter Muscle Volume ( US)    | Masseter Muscle thickness ( US)              | r = -0.91<br>P < .0001**   |
| Masseter Muscle Area ( US)      | Condylion- Gonion (LC)                       | r = 0.81<br>P =0.002*      |
| Masseter Muscle Area ( US)      | Articulare- Gonion (LC)                      | r = 0.85<br>P =0.001*      |
| Masseter Muscle thickness ( US) | Ricketts Measurements ( R1-R2)               | r = 0.82<br>P =0.002*      |
| Masseter Muscle Volume ( US)    | Ricketts Measurements ( R1-R2)               | r = 0.79<br>P =0.004*      |
| Masseter Muscle Area ( US)      | Nasion-Gnathion to Articulare-Gonion         | r = -0.85<br>P =0.001*     |
| Masseter Muscle Area ( US)      | Articulare-Gonion to Gonion-Menton           | r = 0.84<br>P =0.001*      |
| Masseter Muscle Area ( US)      | Ricketts Measurements ( R3-R4)               | r = 0.71<br>P =0.01*       |

**Table 7.2.** Significant correlations and p values for different Ultrasonography (US) and lateral cephalograms (LC) variables. P values with:

\* = significant,

\*\* = highly significant.

| Predictive Equations                                     | $r^2$ | Mean S E |
|--|-------|----------|
| Co-Go = 69.51740 + -3.61031(Thickness) + 0.01322(Volume) | 0.82  | 3.44     |
| Ar-Go = -0.22142 + 0.51323(Length)+0.00354(Volume)       | 0.71  | 3.72     |
| Go-Me = 64.71258 + 0.00275(Volume)                       | 0.41  | 3.38     |
| N-Me = 88.78858 + 1.42912(Thickness)                     | 0.38  | 4.13     |
| N-Gn = 88.10332 + 1.33800(Thickness)                     | 0.31  | 4.51     |
| R1-R2 = 6.38054 + 1.66171(Thickness)                     | 0.68  | 2.56     |
| R3-R4 = 33.42833 + 0.00458(Volume)                       | 0.47  | 4.96     |
| masseter = 23.23336 + 0.51001(Length)                    | 0.33  | 5.18     |

**Table 7.3.** Predictive equations with stars highlighting the significant ones along with standard error of the mean (Mean SE). Volume is significant in most of the predictive equations and provides equivalent cephalometric data.

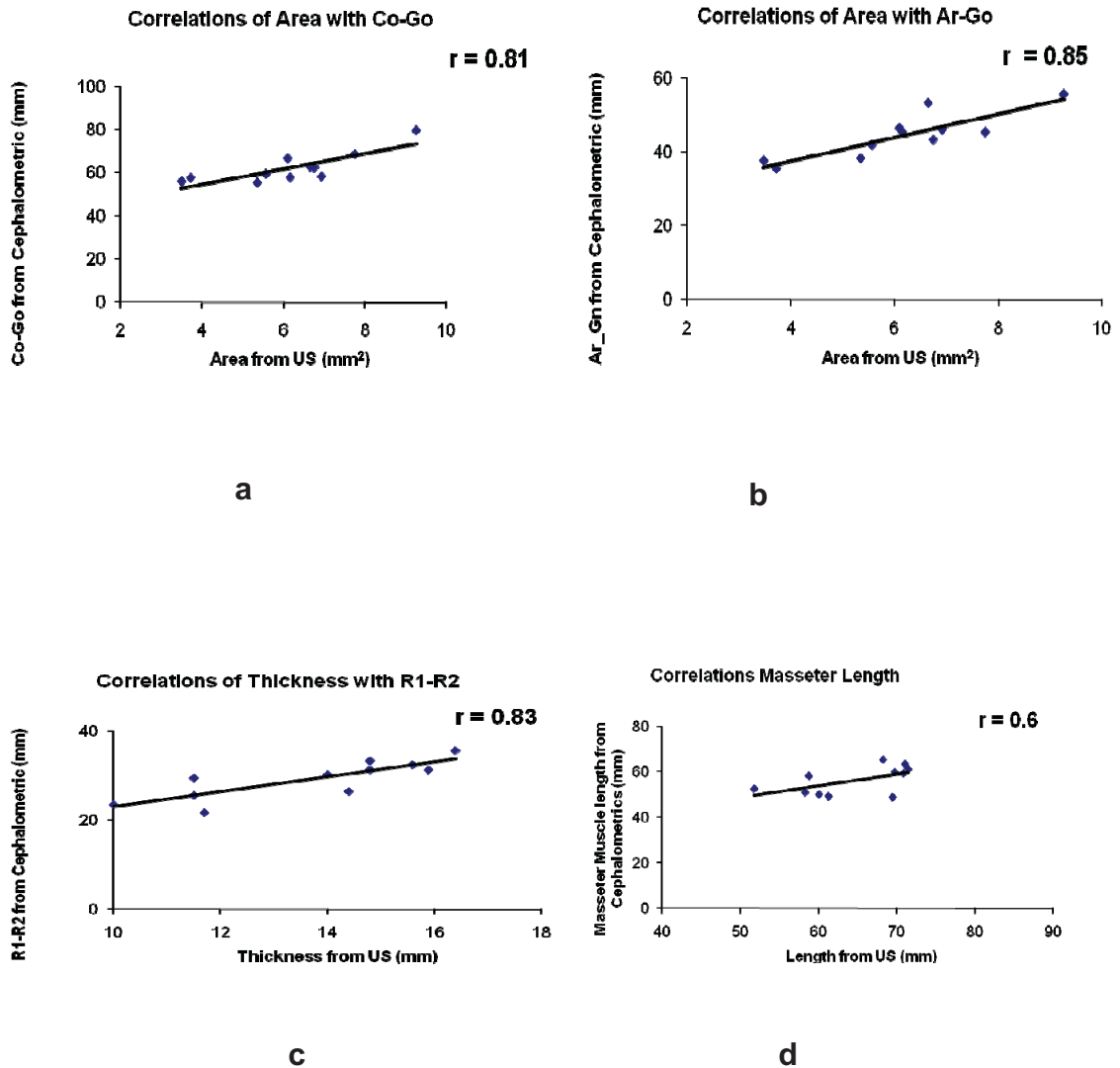


**Figure 7.5:** Statistically significant correlations for area with Co-Go (a) and Ar-Go (b); along with thickness of masseter muscle from US and R1-R2 cephalometric parameters(c). The masseter muscle length (US) and masseter length from cephalometric measurements show modest correlation (d).

## 7.5 DISCUSSION

The present study has used EFOV technology for the first time to assess masseter muscle thickness and length. The image quality using this technology was superior than used in a previous study<sup>17</sup> and could image due to its high frequency and linear array transducer which provides better delineation of the masseter muscle. Although most ultrasound equipment is capable of measuring structures from the imaging display to within 0.1mm<sup>122</sup>, the main barrier to the use of US for periodic orthodontic review is in precise reproduction and accuracy of measurements. This is true for both conventional US and EFOV, but error is magnified with EFOV, similar to 3D US due to the free hand sweep used to acquire images. Although Siescape EFOV technology is specified to produce measurements +/- 2.5% (Siemens Medical Solutions), it is important to verify accuracy in different settings because errors are inherent to the scanning technique, the image reconstruction process and the image measurement method<sup>200</sup>. The pilot study showed that the measurement process was accurate. Our results compared more favourably than those by Close et al<sup>17</sup> who found consistent over-estimation of length compared to cross-sectional area by as much as 25%. The reason for this may have been that although Close et al<sup>17</sup> used a technique that did not necessitate freehand scanning, a lower frequency transducer was used which renders lower imaging resolution despite accurate identification of landmarks which may be an issue. We were careful to demonstrate accuracy of the technique when measuring masseter length with EFOV in our pilot study.

The reproducibility of US measurements in this study was acceptable and similar to earlier reports in the literature<sup>8, 18, 27, 121, 128</sup>. Reproducibility was optimized by measuring contracted rather than relaxed muscles as recommended<sup>207</sup>. A standardised sonographic technique was used by an experienced, single sonographer for all measurements which reduced measurement variability.

Given the accuracy and reproducibility of the US measurements demonstrated in the pilot study, it was surprising that the cephalometric representation of masseter length was only marginally correlated ( $r=0.6$ ,  $p < 0.06$ ) to US measurements of length. The

---

pilot study may have been biased by using lead markers to emphasise the measurement site. Our results may have also been biased by the small sample which was relatively homogenous but contained three subjects exhibiting short face heights. However, thicker masseter muscles generally relate to shorter face heights<sup>27, 107, 128</sup>.

This study found that high positive correlations (Figure 7.5) existed between US measurements for muscle area and cephalometric measurements of superficial muscle length approximation (Co-Go,  $r=0.81$ ,  $p < 0.002$ ) ; (Fig 7.5 a), and mandibular length (Ar-Go,  $r=0.85$   $p < 0.001$ ) ; (Fig 7.5 b). These results were similar to a 3D US study<sup>200</sup> and a recent MRI study MRI<sup>156</sup> which also demonstrated strong correlations between vertical face heights and masseter muscle thickness and volume. These findings suggest that US measurements of masseter area, thickness and volume could be used to predict vertical face heights.

Gonial angles, both upper and lower, along with ODI are considered important assessment variables for vertical facial proportions and directions of growth<sup>199</sup>. However, the present study found no statistically significant relationship between these cephalometric measurements and US length, thickness, area or volume. Nevertheless, predictive equations for cephalometric variables derived from the US measurements can provide information beyond the measurements of length, area, thickness and volume alone.

Measurements of masseter muscle thickness (mean 13.69 mm $\pm$  2.15) were comparable to similar documented measurements (range 11mm to 16.7mm)<sup>122</sup>. Muscle volume appears more variable, exhibiting a larger standard deviation (Table 7.1) than the mean. This may perhaps be attributed to volume being calculated mathematically, which may be a source of error in translating to true biological shape and dimensions for masseter muscle. For volume derivations, 3D US scans will still be required<sup>200</sup>. A 3D US study<sup>200</sup> and a recent study with MRI<sup>156</sup> have shown a strong correlation between vertical face heights and masseter muscle thickness and volume. The accuracy and precision of US measurements of masseter muscle length, thickness area and volume may improve with further technological refinements.

This preliminary study has used simple imaging US techniques to investigate possible relationships with multiple cephalometric facial skeletal measurements. Equations were derived which could potentially predict certain cephalometric variables from US measurements, particularly mandibular ramus dimensions. Such predictions would be desirable to reduce radiation exposure when serial evaluations on individuals are required. Future work should optimise the accuracy and reduce error in US measurements, while prediction equations need validation with larger and more diverse sample populations. Currently, the utility of US for mainstream orthodontic treatment planning is unproven but holds great promise for the future.

#### 7.5.1 ACKNOWLEDGEMENTS

We appreciate the funding provided by the Australian Dental Research Foundation and Dr J Fricker, Tidbinbilla, Canberra, ACT Australia and Dr.S Vallance, senior research officer, Mona Lisa Imaging ([scott@monalisaimaging.net](mailto:scott@monalisaimaging.net)). Our sincere thanks go to the staff at UniSA for their collaboration with the project, Dr Nancy Briggs (The University of Adelaide) for statistical analyses and Mrs Lucy Hatch for secretarial assistance.

(This paper will be submitted to the  
American Journal of Orthodontics and  
Dentofacial Orthopedics)

## 8 ANALYSIS AND CORRELATIONS OF HUMAN MASSETER MUSCLE WITH 3D IMAGING, ULTRASONOGRAPHY AND LATERAL CEPHALOMETRICS

SHAZIA NASER-UD-DIN <sup>a</sup>, KERRY THOIRS <sup>b</sup>, CRAIG DREYER <sup>c</sup>,  
WAYNE SAMPSON <sup>d\*</sup>

Adelaide, SA, Australia

- a** PhD Candidate Orthodontics (University of Adelaide, Australia), BDS, DPH Dent, MSc (Ortho) DCPSP – HPE, FICCD Orthodontic Unit, School of Dentistry, University of Adelaide
- b** PhD, MMedRad, AMS, School of Health Sciences, University of South Australia
- c** PhD, MDS, BDS, MRACDS (Orth) FRACDS, FICD, GCertEd (HE), Orthodontic Unit, School of Dentistry, University of Adelaide
- d** BDS, BSciDent (Hons), MDS, FDSRCS (Eng), FICD, FADI, Begg Chair, Orthodontic Unit, School of Dentistry, University of Adelaide

### Reprint requests to :

Prof WJ Sampson, Begg Chair, Orthodontic Unit, School of Dentistry, The University of Adelaide,  
Adelaide, SA 5005, [wayne.sampson@adelaide.edu.au](mailto:wayne.sampson@adelaide.edu.au)

## 8.1 ABSTRACT

### INTRODUCTION

Orthodontic diagnosis requires accurate, reliable dento-facial analysis which should preferably be 3D, non-invasive, cost-effective and user-friendly. With growing concern regarding exposure to ionizing radiation over the course of treatment, 3D facial imaging and characterization of muscle form with ultrasonography (US) without sequential radiographs could provide useful information during growth, development and treatment periods. Furthermore, mathematical models of varying complexity have been developed to maximize the information from the available investigative system.

### METHODS

Eleven volunteers (8 females; age range 22-30 years) were recruited for US and standard lateral radiographs measurements along with 3D imaging ( $n=10$ ) using a structured light technique. The three investigations were done to assess the vertical and transverse dimensions of the face along with superficial masseter muscle dimensions. In total, 33 variables were analysed.

### RESULTS

Pearson correlation coefficients showed highly significant correlations intra-investigation particularly between lateral cephalometric and ultrasonography variables  $r=0.92$  ( $p=0$ ) and  $r=0.95$  ( $p=0$ ) respectively. Strong correlations were also observed with Co-Go and masseter muscle area derived from ultrasonography  $r=0.81$  ( $p=0.01$ ). Similarly, strong correlations were seen between Go-Me to facial width from 3D imaging  $r=0.83$  ( $p=0.003$ ). A high statistical significance ( $p < 0.0001$ ) for curvilinear measurements compared with the linear counterparts was revealed with paired t-tests. Factor analyses suggested interrelationships for generation of predictive equations for lateral cephalometric variables deduced from 3D image coordinates.

### CONCLUSION

This preliminary investigation suggests that potentially useful clinical information can be gathered without repeated exposure to ionizing radiation. For more robust predictive equations, a larger study would be required to validate such a model.



## 8.2 INTRODUCTION

Assessment and treatment planning in orthodontics has traditionally been based on two dimensional representations such as lateral cephalograms and facial photographs. Hence, precision and the ability to account for subtle changes over the course of growth or treatment, particularly in the soft tissues, have been lacking. This was aptly referred to as the “*flat earth concept*” by Clark<sup>148</sup>. However, new additions to the orthodontic armamentarium<sup>149</sup> need to be cost-effective, user-friendly and not undermine patient comfort or compliance. Form and function are complexly interrelated and no orthodontic diagnosis would be complete without a proper functional assessment. Of course, this might be easier said than done as functional recordings can be time intensive and difficult to validate<sup>98</sup>. US and EMG have been used for recording muscle changes and reflexes in varying facial proportion individuals, respectively. Moreover, if comprehensive information could be gained through mathematical models limiting the number of investigations it would improve overall efficiency in diagnosis, treatment planning and evaluation.

Pioneering work in anthropometric facial assessment was carried out by Farkas<sup>126</sup> who paved the way for facial measurements with 3D scanning. Farkas is credited with promoting anthropometry which has an advantage over 3D imaging due to the ability to palpate bony landmarks underlying the soft tissue. However, a well-known limitation of anthropometry is the cooperation level required while measurements are taken, particularly with young subjects<sup>208</sup>. Moreover, anthropometric measurements are confounded by the variability of soft tissues, head orientation and examiner subjectivity<sup>208</sup>.

The transverse dimension is an important variable that can be analysed by anthropometry or 3D techniques<sup>155</sup> as assessment is not available through routine lateral cephalometric analyses. Obviously, the physiognomy of the face is influenced by the skeletal pattern and the relationship of lateral cephalometric norms and facial measurements has been studied extensively<sup>209</sup>.

Several indices (in Methods) provide ratios for vertical and transverse facial proportions where comparison among subjects is more easily performed without the need for factoring facial size differences.

### 8.2.1 3D IMAGING

3D imaging has rapidly progressed in recent years, particularly after its introduction six decades ago by Thalmann-Degen, in Burke<sup>210</sup>. Primarily developed for application in industry<sup>132, 211</sup>, there are various types of imaging techniques including stereo photogrammetry<sup>140</sup>, 3D laser scanning, vision-based scans (Moiré tomography) along with the latest, safest and most cost-effective structured light 3D imaging<sup>108</sup>.

Structured light creates a superficial, shell-like reproduction of the face enabling the digitized topology of the face to be displayed in 3D. It is considered a very safe and cost-effective way of producing 3D images. However, like any other system it is subject to error which depends on a number of different factors; particularly, the level of background light, the level of the projected light and the distance to the subject<sup>143</sup>. The way these factors interact can complicate the error level which is calculated by scanning a target containing patterns of known dimensions.

### 8.2.2 ULTRASONOGRAPHY

Ultrasonography (US) is considered as a safe, non-invasive, cost-effective and comfortable diagnostic tool. Good high resolution images of soft tissues are obtained by US which have been claimed to be superior to MRI and CT scans<sup>8</sup>. Exciting future applications such as “*Virtual biopsies*” with the acoustic scanning microscope provide new high-resolution imaging capabilities with US<sup>202</sup>.

US can be utilized in orthodontics to supplement radiographic diagnosis of facial patterns<sup>8</sup>, particularly when repeated radiation dose is of concern in growing individuals. However, US is already finding use in clinical applications to monitor condylar translations in post-orthognathic surgery cases<sup>212</sup>, assessment of disc displacements<sup>213</sup>, and screening for juvenile idiopathic arthritis<sup>106</sup>. Real time US can

be used to determine soft tissue function (e.g tongue position at rest, speech and swallowing) before during and following orthodontic or orthognathic treatment<sup>214</sup>.

### 8.2.3 LATERAL CEPHALOMETRICS

Lateral cephalometric techniques have been the mainstay for orthodontic, orthognathic and dentofacial growth studies for over seven decades. However, this useful tool has two major limitations. Firstly, the cumulative radiation dosage from successive films and, secondly, the two-dimensional image is a distorted representation of the three-dimensional craniofacial region. The latter, in particular, is of significance as the complex shapes of the craniofacial region are poorly represented. Hence, the measurement and valid description of the head is limited by landmark error, reference plane and area selection. Trpkova<sup>115</sup> in a recent meta-analysis found a limited number of landmarks with high reproducibility. Alternative methods suggested by Hurst include mathematical models that enhance the descriptive accuracy of complex shapes and increase the overall validity of the measurements, such as linear, angular and proportional, conventionally adapted for cephalograms<sup>215</sup>. Mathematical models include Euclidian distance matrix<sup>216</sup>, thin plate spline graphical analysis, finite element morphometry<sup>217</sup> and Fourier analysis of cephalometric shapes<sup>218</sup>, to cite just a few. The major issue with such analyses is this complexity and lack of acceptance.

The aim of the present study was to analyse and correlate facial data derived from three different imaging sources: 3D surface imaging, lateral cephalometrics, and ultrasonography. Furthermore, relationships that might be translated into future mathematical models were evaluated.

## 8.3 SUBJECTS AND METHODS

Eleven volunteers (age range 22-30 years; 8 females) were recruited for the ultrasonography study but one male participant did drop out for the 3D imaging. Approval was obtained from by the Human Ethics committees of The University of Adelaide and University of South Australia and conformed to the Helsinki Declaration. All had a natural, healthy dentition free from dental diseases and with no overt temporomandibular disorders. Written information was provided and consent obtained and each participant was aware of their rights to withdraw at any stage.

### 8.3.1 EXPERIMENTAL SET-UP

### 8.3.2 3D IMAGING

Each subject was requested to sit comfortably on a back supporting chair, in natural head posture, and in a well-lit room. Instructions were given to keep the eyes open, if possible, and to have the hair pinned back so that the face could be imaged without any disturbance or noise.

A structured light projector was placed 1.5 metres from the subject and a horizontal light grid was flashed for one second (Fig. 8.1). Two frontal images were taken along with one left side profile image. The system used in this study comprised a BENQ DLP projector (Dell Computers, Dallas, TX, BenQ Corporation Hsinchu, Taiwan, Dell Inspiron laptop (Taipei, Taiwan) and two cameras (Firefly MV, Point Grey Research (Richmond, BC, Canada). The structured light system produced a 3D image by emitting light in a known pattern and capturing these images with dual cameras. The 3D locations of the points in the captured image can be calculated with triangulation. Triangulation, requires the relative location of the camera and projector to be known. Calibration of the light emitting projector was used to determine the relative locations of the camera(s) by scanning a target with a checkerboard pattern of known size multiple times from different points of view. At least five different scans are needed to successfully calibrate the scanner but, for the purpose of increased accuracy, 20 scans were performed.

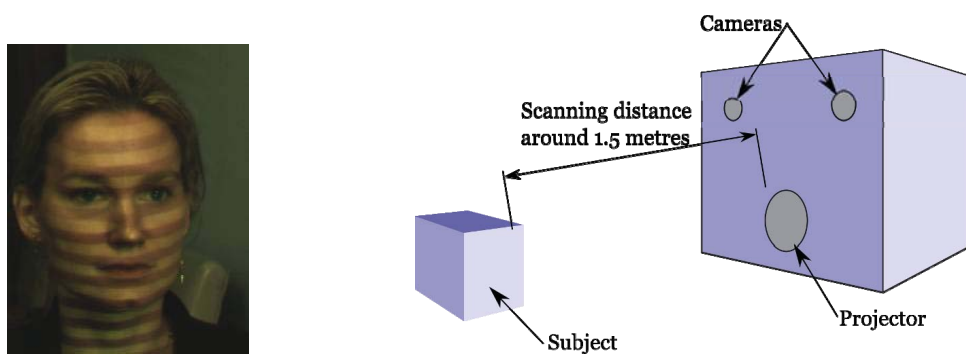


**Fig. 8.1.** Capturing an image with the 3D structured light projector placed 1.5m from the subject. The grid of light with horizontal pattern is flashed on the subject's face for 1sec. Triangulation helps to generate the 3D effect. (Permission obtained from subject, see appendix)

Each scan was captured in approximately one second and the data were processed for 30 seconds by the computer to perform the triangulation. The raw scans of the subjects produced around 200,000 3D points, which were further processed in Vr Mesh (software package for processing Point Clouds which is available at : <http://www.vrmesh.com/>) for the raw data to remove unwanted background scanned data and noise. Each scan had the area of interest manually extracted from the raw scan and then uniformly re-sampled which detected removed points in order to achieve a constant distance between remaining points. The re-sampled scans were de-noised with a filter and converted into a 3D meshwork of triangles for measurement.

### 8.3.3 3D IMAGE ANALYSES

The images were analysed on Meshlab software (from <http://meshlab.sourceforge.net/wiki/index.php/Developers> linked to The Italian National Research Council's website <http://www.isti.cnr.it/>) (Fig. 8.2). Software landmarks were identified by one operator (SND) and to enable best positioning, the image was magnified and rotated and points were entered for soft tissue glabella (g), nasion (n), gnathion (gn), subnasale (sn) tragus (t), gonion (go), zygonion (zy), pogonion (pg) orbitale (or) and stomion (st)<sup>126</sup> (Fig. 8.2).

The variables selected were from Farkas<sup>126</sup> and were generated by default analysis programs. They were broadly classified as linear, angular and proportional (Table 8.1 a)

|    | Symbol | Landmark  | Definition  |
|----|--------|-----------|---|
| 1  | n      | Nasion    | Midline at the junction of nasal root and nasofrontal suture above the inner canthi               |
| 2  | g      | Glabella  | Most prominent midline point between eyebrows   |
| 3  | sn     | SubNasale | Midpoint of the columella crest   |
| 4  | gn     | Gnathion  | Median lowest landmark on the bony chin   |
| 5  | or     | Orbitale  | Lowest point on lower margin of orbit   |
| 6  | pg     | Pogonion  | Anterior most midpoint of the chin  |
| 7  | sto    | Stomion   | point at the crossing of vertical facial midline with horizontal labial fissures                  |
| 8  | t      | Tragion   | Notch at the upper margin of the tragus   |
| 9  | go     | Gonion    | Lateral most point on the mandibular angle  |
| 10 | zy     | Zygion    | Lateral most point of each zygomatic arch, similar to the zygion of the malar bone (l= left side) |

**Table 8.1 (a)** Landmark abbreviations and definitions of 3D points as defined by Farkas<sup>126</sup>.

|    | Symbol | Landmark                 | Definition  |
|----|--------|--------------------------|---|
| 1  | N      | Nasion                   | Radiolucent delineation at the frontonasal suture at the junction of the frontal bone and nasal cartilage |
| 2  | S      | Sella                    | Central point of the sella turcica in the sphenoid bone   |
| 3  | Or     | Orbitale                 | Average lowest point on the bony border of the orbits   |
| 4  | Po     | Porion                   | Machine Po at the most superior point from the ear rod of the cephalostat                                 |
| 5  | ANS    | Anterior Nasal Spine     | Most anterior tip of the bony maxilla   |
| 6  | PNS    | Posterior Nasal Spine    | Most posterior limit of the bony maxilla  |
| 7  | A      | Point A                  | Deepest point on the anterior curvature of the maxilla between anterior nasal spine and supradentale      |
| 8  | B      | Point B                  | Deepest point on the symphyseal outline between infradentale and pogonion                                 |
| 9  | Ptm    | Pterygomaxillary fissure | Most inferior point on the inverted tear drop outline of the pterygomaxillary fissure                     |
| 10 | Go     | Gonion                   | Midpoint of the angle of the mandible   |
| 11 | Co     | Condylion                | Most posterior superior point on the outline of the condylar head   |
| 12 | Ar     | Articulare               | Intersection of cranial base image with posterior border of the mandibular condyles                       |
| 14 | Pog    | Pogonion                 | Most anterior point on the bony chin  |
| 15 | Me     | Menton                   | Most inferior point on the bony chin  |

**Table 8.1 (b)** Lateral cephalogram landmarks as defined in Trpkova *et al.*<sup>115</sup>



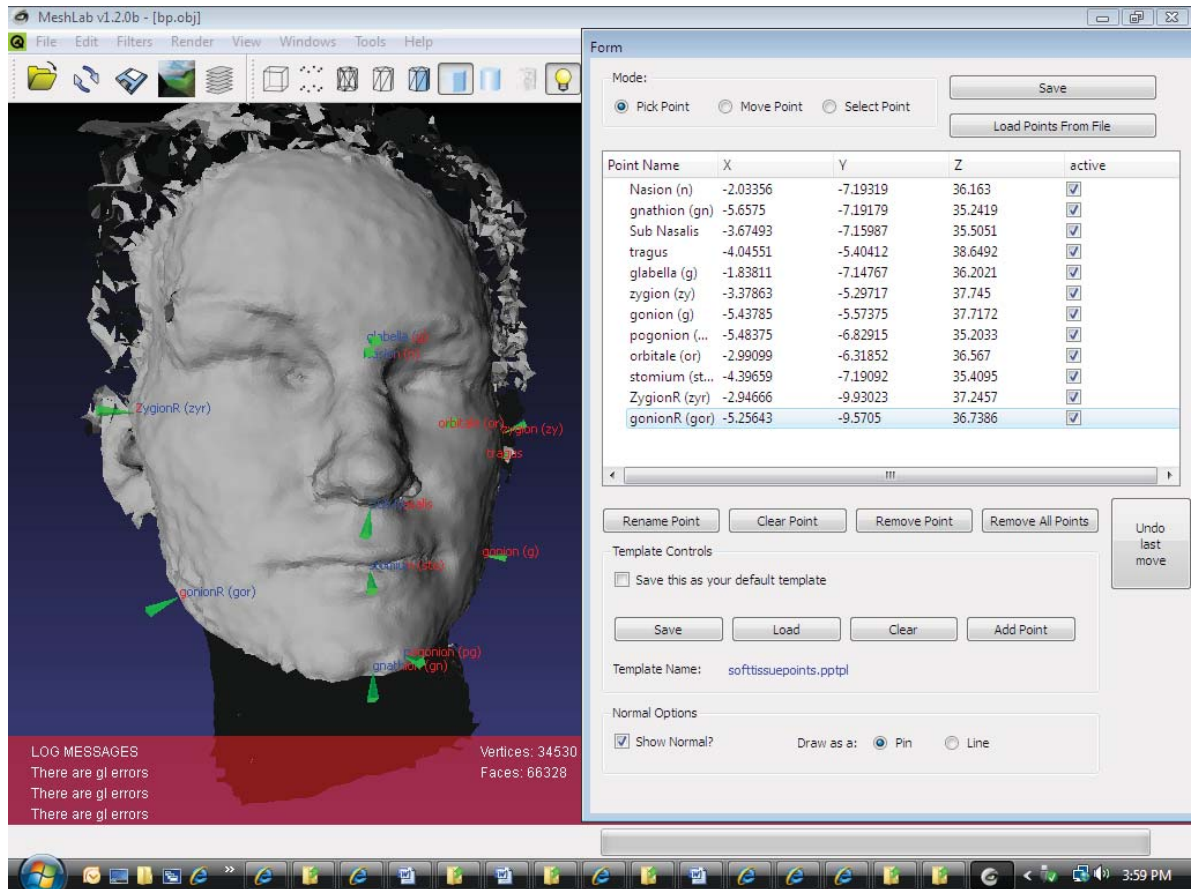


**Fig. 8.2.** Analysis of 3D scanned images using MeshLab® shows point selection for computing distances between the landmarks.

### 8.3.4 3D LINEAR MEASUREMENTS

Nine linear measurements were made on each 3D image. Face height was measured from nasion to gnathion (n-gn) in Fig.8.3, while mandibular height was measured from stomion to gnathion (sto-gn).

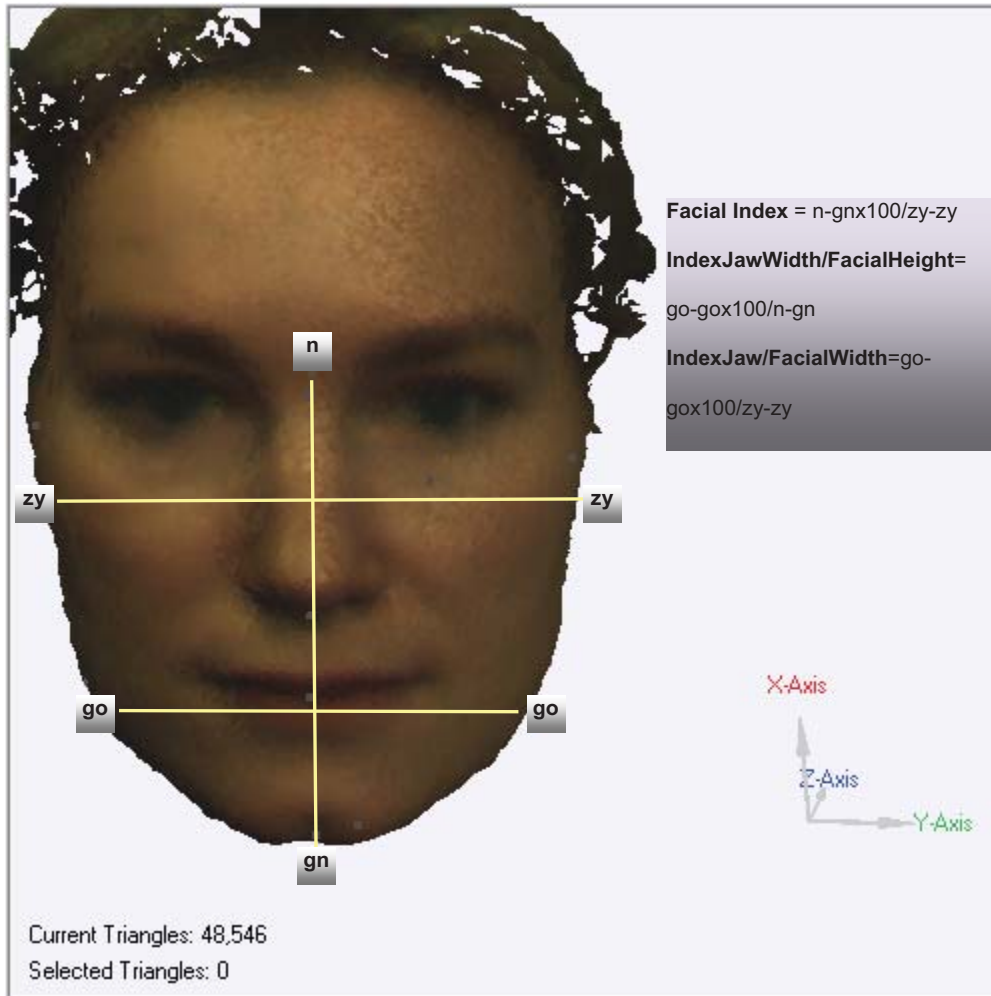


**Fig. 8.3** Anthropometric Indices of Farkas<sup>126</sup> applied to 3D images for transverse and vertical assessments.

### 8.3.5 3D TRANSVERSE DIMENSIONS

The bizygion diameter (zy-zy) represents the transverse dimension of the upper face width, at its widest part. The 3D scan was rotated right and left for determination of the most lateral point on the zygomatic arch. Even though palpation would be preferred, the scans had a distinct shadow that assisted in zy recognition. The bigonial diameter (go-go) represents the width of the lower face (Fig. 8.3).

### 8.3.6 3D PERPENDICULAR MEASUREMENTS

Perpendicular measurements were generated from midline landmarks; nasion (n), subnasale (sn), stomion (sto) and gnathion (gn). Face height was measured from nasion to gnathion (n-gn) (Fig. 8.3) and mandibular height from stomion to gnathion (sto-gn)<sup>126</sup>.

### 8.3.7 3D TANGENTIAL/ CURVILINEAR MEASUREMENTS

The curvilinear measurements were included to enhance the data and find out if there was any significant difference with corresponding linear measurements (Fig.8.4).

The mandibular curvilinear arc extended from right tragus to subnasale to left tragus (t-sn-t). The tangential mandibular depth was measured from tragus to gnathion (t-gn) from the left aspect only for consistency with US scans. A second angular measurement was generated from tragus to gonion (t-go) and gonion to gnathion (go-gn) defined as the mandibular inclination<sup>126</sup>. This was another way to express lower vertical dimensions.

### 8.3.8 3D INDICES

Overall six indices were used:

|                                       |                             |
|---------------------------------------|-----------------------------|
| 1. Facial Index                       | $n-gn \times 100 / zy-zy$   |
| 2. Jaw Index                          | $sto-gn \times 100 / go-go$ |
| 3. Index of jaw /facial width         | $go-go \times 100 / zy-zy$  |
| 4. Index of jaw width / facial height | $go-go \times 100 / n-gn$   |
| 5. Index of lower jaw / facial height | $sn-gn \times 100 / n-gn$   |
| 6. Index of jaw / face height         | $sto-gn \times 100 / n-sto$ |

These represented the vertical and transverse proportions both in mid-face and lower jaw regions some of which are depicted in Fig. 8.3 <sup>126</sup>.

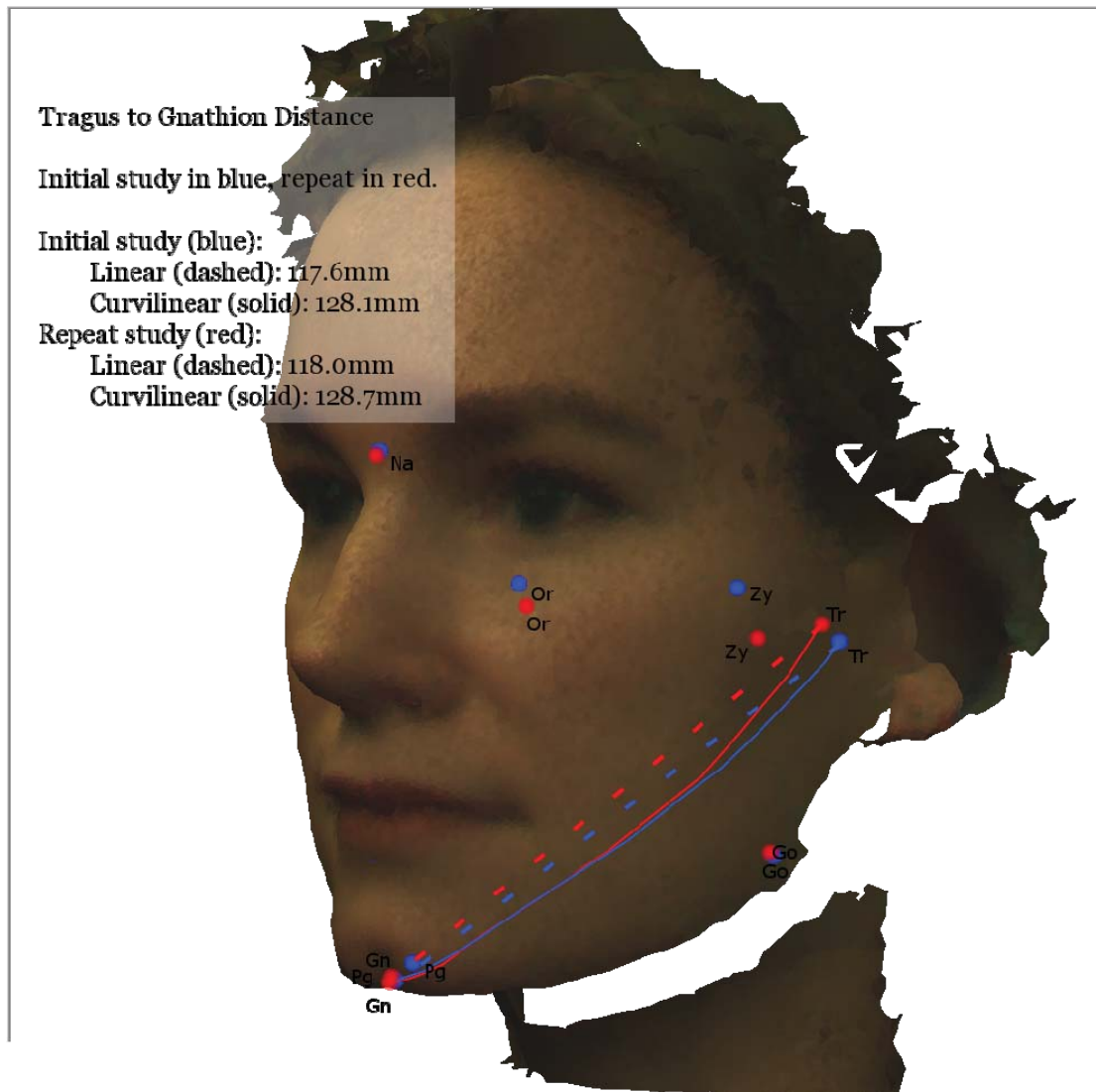


**Fig. 8.4** Curvilinear and linear mandibular measurements for the left side of the subject. There is a clear advantage with 3D images over photographs.

### 8.3.9 ULTRASONOGRAPHY (US)

US scans were conducted in a semi-darkened room by an accredited sonographer (KT). Light hand-held pressure, which is a routine recommendation,<sup>121</sup> was used and left side measurements were taken for consistency with previous work<sup>204</sup>. Masseter muscle images were produced at the University of South Australia using a Siemens

Antares Sonoline ultrasound machine (Siemens Medical Solutions, USA Inc, Ultrasound Group, Issaquah WA) and a 5-13 MHz linear array transducer Siescape ® technology (Siemens Medical Solutions, USA Inc, Ultrasound Group, Issaquah WA) was used to produce freehand EFOV (Extended Field of View) images, whilst maintaining the transducer orientation perpendicular to the mandible. EFOV imaging allowed complete imaging of the masseter muscle, even though the muscle was longer than the length of the face of the ultrasound transducer. The accuracy of linear measurements from images acquired with Siescape ® technology is specified to +/- 5% or 2.5mm whichever is greater (Siemens Medical Solutions, (2001) Sonoline Antares Ultrasound Imaging System. Instructions for Use, Siemens Medical Solutions, Issaquah, USA) (Fig. 8.5 a & b).

The image plane extended between the zygomatic tubercle and gonial angle. Subjects were requested to clench in intercuspal position for 10-15sec. Measurements were made using electronic calipers inherent in the US system for length, thickness and cross-sectional area. Length of the masseter muscle was measured as the distance between the zygomatic tubercle to the gonial angle for superficial masseter. The thickness was measured as the maximum distance between the superficial and deep aspects of the masseter muscle while the cross-sectional area was traced manually on the depicted boundaries of the muscle (Fig. 8.5b).

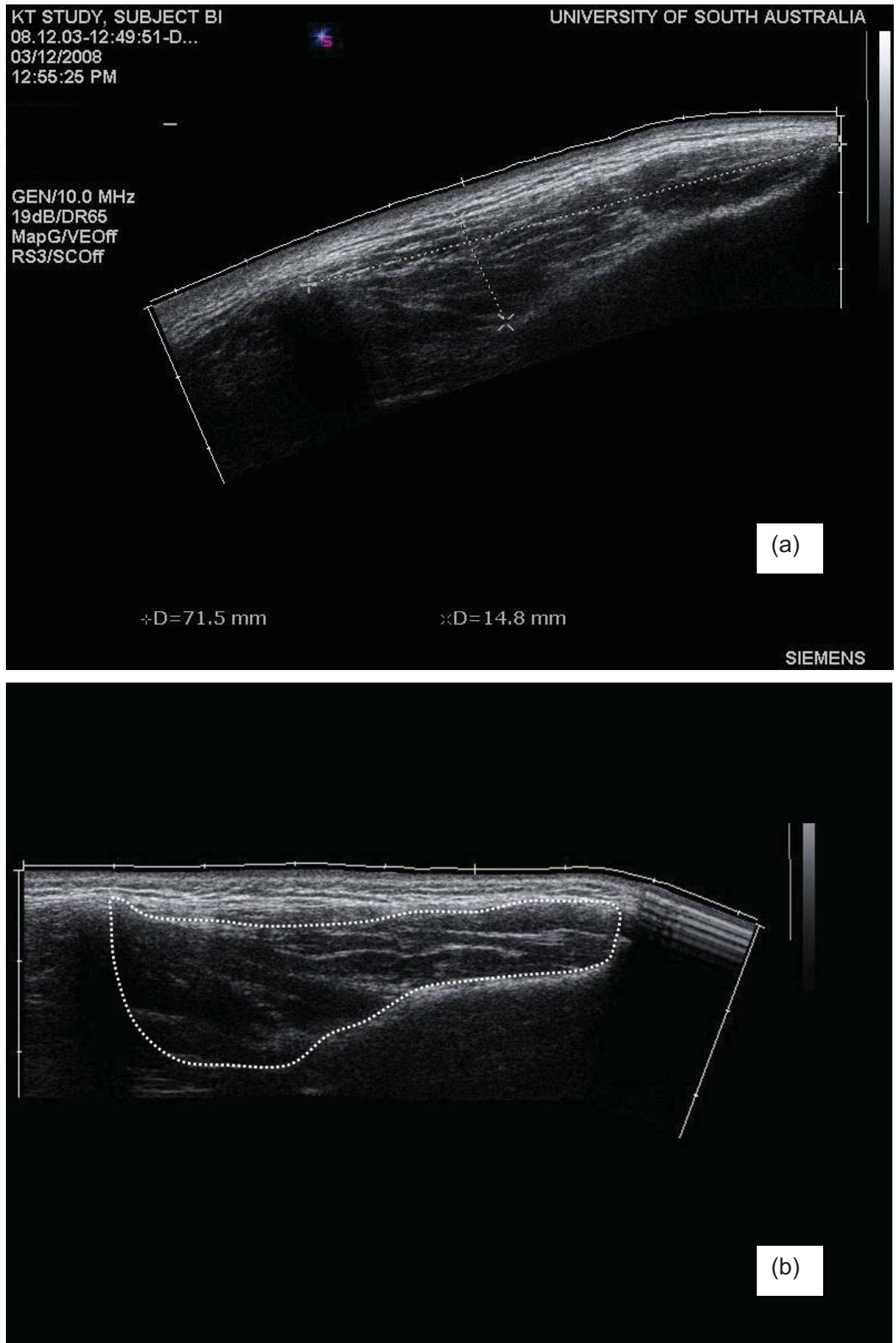


**Fig.8.5** US of left masseter with length and thickness (a) along with area (b) outlined on screen after scanning.

### 8.3.10 LATERAL CEPHALOGRAMS

Each subject had a standard lateral cephalogram taken with a magnification factor of 1.083 with the Siemens Nador 2 SR system (Bensheim, Germany) with specifications of 220V, 50 Hz and 10amp. The focus-film distance was 150cm and mid-sagittal plane- film distance was 11.5cm. The exposure time was 0.64sec with 75kv and 20mA.

Dolphin<sup>®</sup> (Los Angeles, California, USA) and Mona Lisa<sup>®</sup> (Tidbinbilla, Canberra, Australia) cephalometric analysis software systems were used to evaluate linear, angular and proportional facial skeletal variables by digitizing scanned images of the lateral cephalograms (Table 8.1 b).

Cephalometric tracings were also performed on standard acetate paper (3M Unitek, Orthodontic Products, Monrovia, CA 91016, USA) with a 0.3mm graphite mechanical pencil in a darkened room for masseter muscle length evaluation only. All tracings and digitization were done by a single investigator (SND).

### 8.3.11 LINEAR CEPHALOMETRIC MEASUREMENTS

The linear measures (Fig. 8.6a) selected were: ramal length, Articulare-Gonion (Ar-Gn) giving the mandibular length; nasion-menton (N-Me) giving the anterior face height; gonion-menton (Go-Me) assesses the mandibular body length; and nasion-gnathion (N-Gn) indicating anterior vertical face height<sup>197</sup>; R1-R2 and R3-R4 represent the ramus shape<sup>205</sup>; and ante-gonial notch (AGoNotch) which is an indicator of mandibular growth rotation and also relates to the facial vertical dimension<sup>130</sup>; and masseter length from the zygomatic tubercle to gonion angle representing attachment points for the superficial masseter muscle<sup>31, 120</sup>. The masseter lengths were measured manually with digital calipers.

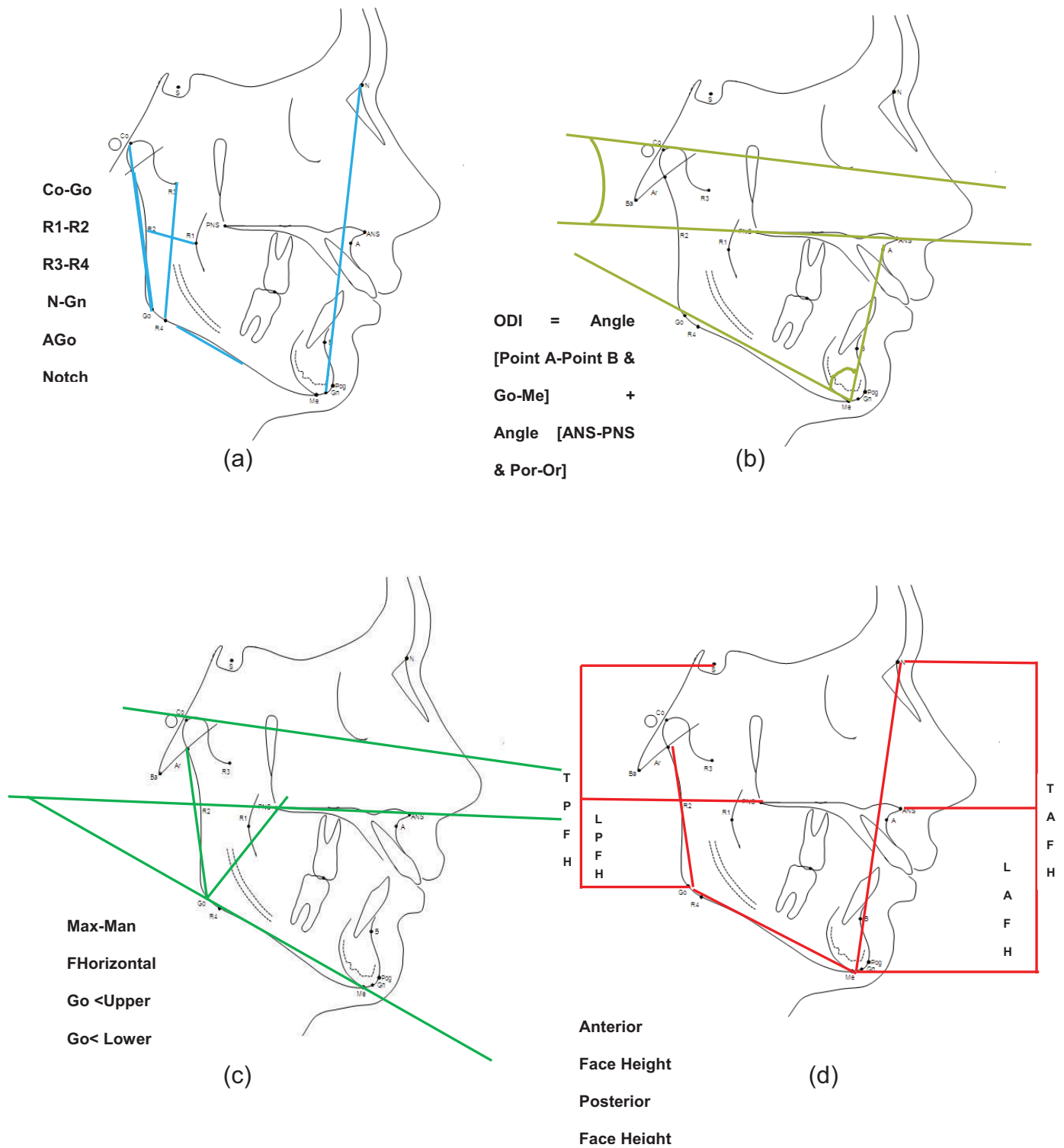


**Fig. 8.6** Lateral cephalometric variables for linear measurements (a), ODI (b), angular (c) and proportional indices (d).



### 8.3.12 ANGULAR CEPHALOMETRIC MEASUREMENTS

Angular variables selected in the study were: gonial (Go angle), upper gonial angle (UGo angle), lower gonial angle (LGo angle), Overbite Depth Indicator (ODI)<sup>199</sup>, maxillo-mandibular planes angle<sup>200</sup>, and Frankfurt Horizontal-Mandibular plane angle (Fig. 8.6 b, c)

### 8.3.13 CEPHALOMETRIC INDICES

The proportional vertical relationships measured were: nasion-gnathion divided by articulare-gonion (NGn/ArGo); anterior lower face height (LAFH/TAFH); and posterior lower face height (LPFH/TPFH)<sup>25, 200</sup> which reflected the anterior and posterior vertical proportions; articulare-gonion by gonion-menton (ArGo/GoMe); and Jarabak Ratio (NMe/GoAr)<sup>219</sup> (Fig. 8.6d).

### 8.3.14 STATISTICS

Basic descriptive statistics with mean, standard deviations and range for 3D images, US and lateral cephalometric variables (Table 8.2) were generated with statistical package SAS 9.1 (SAS Institute, Inc. Cary, NC. USA). Although a small sample size, it was considered normally distributed and treated likewise. Pearson correlation coefficients of a total of 26 variables from the three experimental settings were assessed. Confidence interval was set at 95%. Repeatability was assessed with Dahlberg's statistic and Bland and Altman method<sup>167</sup>.

### 8.3.15 ERROR METHOD

Errors in a structured light scan can manifest as either a scaling error or as an absolute error. Scaling errors are best expressed as percentages and for the Mona Lisa® Imaging system (Tidbinbilla, Canberra, Australia) the mean error is 0.39% with a standard deviation of 0.31%. At larger distances measurement scaling errors will dominate but for measurements under 150mm the error is better expressed as a constant with a mean of 0.53 mm and a standard deviation of 0.44 mm. Generally the

repeatability is higher with 3D laser scanning images which are of the order of 0.66%<sup>152</sup>. More accurate scans are obtained from the frontal view<sup>141</sup> which was chosen for the present study.

Factor analysis was conducted due to the large number of variables and Eigenvalues were produced. A total of 33 variables from 12 lateral cephalometric, 17 from 3D scanning and four from US were analysed. For US and lateral cephalogram recordings repeats were done on the entire sample at two separate interval five weeks apart and statistically assessed with Bland and Altman and Dahlberg's statistics.

### 8.3.16 PREDICTIVE EQUATIONS

With regressions and significant correlations, predictive equations were produced to substitute lateral cephalometric measurements. The factors would provide the basis of meaningful interrelationships.

## 8.4 RESULTS

Descriptive statistics (Table 8.2) show the mean and standard deviations for linear, proportional and angular variables taken from 3D imaging and lateral cephalograms. Even though the sample size was relatively limited the distribution of the data was normal.

Reproducibility of landmarks and indices was checked with Dahlberg's statistics (Table 8.5) and the Bland and Altman method (Fig. 8.7a &b). Generally, the reproducibility was within the acceptable range with the occasional exception of an outlier such as depicted in Jaw/ Facial height index (Fig. 8.7 a). Since there were three co-ordinates x, y and z separate analyses were done for each independent landmark with standard error and sum of error presented in Table 8.6.

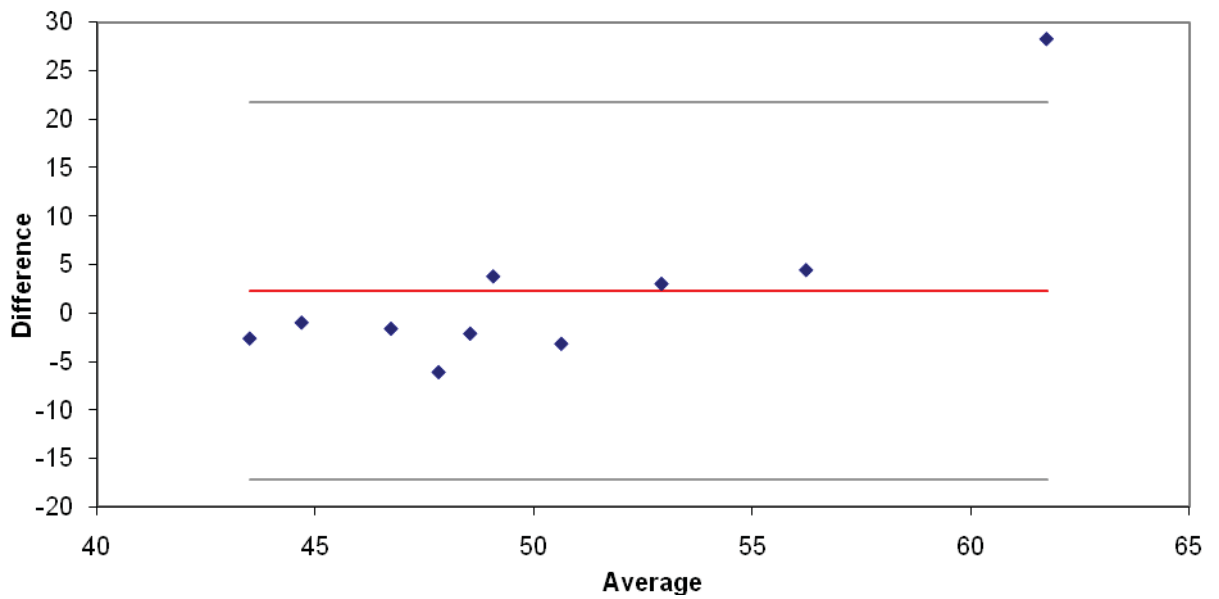


**Fig. 8.7 (a)** Bland and Altman plot for Index of Jaw / Facial height with good reproducibility exception with an outlier on the far upper right corner.

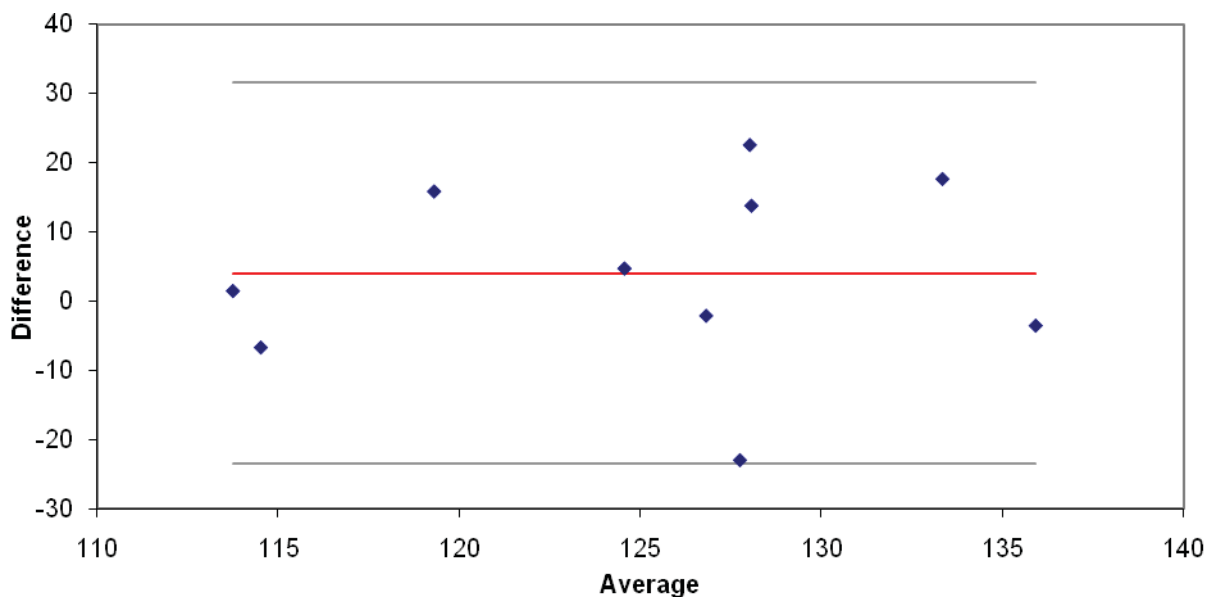


**Fig. 8.7 (b)** Example of large spread in Index Jaw/ Facial Width and poor reproducibility with the Bland and Altman method.

We found significant correlations (Table 8.3). Interrelated cephalometric variables showed the highest correlations; for example Co-Go with Ricketts R3-R4 where  $r=0.92$  ( $p=0$ ). Likewise, in US volume and thickness had  $r=0.95$  ( $p=0$ ). Inter-investigatory high correlations were found for Ar-Go from lateral cephalograms with the Jaw Index from 3D imaging  $r=0.86$  ( $p=0.001$ ). An important correlation was t-go (3D) correlation with Co-Go (cephalometric) being  $r=0.76$  ( $p=0.01$ ). Interestingly, face width (3D) and masseter length from lateral cephalometrics had good correlation  $r=0.78$  ( $p=0.001$ ). These variable correlations could well be used in lieu of each other. Only moderate correlations were present among US and 3D images (Table 8.3 and 8.4). The ODI generally had a low and inverse correlation with US and 3D imaging variables (Table 8.3). However, it showed strong correlation with lateral cephalometric variables.

Two rotated factor patterns were generated from Factor Analysis for US which were then correlated to linear, angular, proportional lateral cephalometric variables and four factors of 3D variables constituting the 3D linear, 3D proportional, 3D Linear width and 3D proportional width (Table 8.7). Factor 1 constitutes thickness and volume of masseter muscle while Factor 2 is length and area of masseter muscle. Reproducibility of lateral cephalometric manual tracing for masseter muscle was satisfactory with 1.1 for the Dahlberg statistic (DS). Similarly, it was within acceptable range for US where for masseter muscle area= 1.1, length= 1.3 and thickness=1.2 (DS). Curvilinear measurements were significantly different ( $p < 0.0001$ ) when compared with linear according to paired t-test.

|                           | <b>Linear</b>                 |                  | <b>Proportional</b> |                                |                            | <b>Angular</b> |   |                      |      |
|---------------------------|-------------------------------|------------------|---------------------|--------------------------------|----------------------------|----------------|---|----------------------|------|
|                           | Variable (mm)                 | Mean             | SD                  | Variable                       | Mean                       | SD             | Variable (°)                                  | Mean                 | SD   |
| <b>3 D Imaging</b>        | Face height                   | 115.9            | 7.2                 | Index lower jaw/face height    | 51.8                       | 2.4            | Mandibular inclination                        | 56.6                 | 10.4 |
|                           | Mandibular height             | 41.6             | 6.1                 | Index jaw / face height        | 51.3                       | 10.0           |   |                      |      |
|                           | Mandibular depth linear       | 116.5            | 12.6                | Facial Index                   | 83.8                       | 6.6            |   |                      |      |
|                           | MandibularDepth Curvilinear   | 123.5            | 13.8                | Jaw Index                      | 32.3                       | 4.2            |   |                      |      |
|                           | Tragus-gonion                 | 44.8             | 7.5                 | Index jaw/ Facial width        | 87.5                       | 5.5            |   |                      |      |
|                           | Gonion-gnathion               | 85.9             | 8.4                 | Index Jaw width/ Facial height | 104.6                      | 5.8            |   |                      |      |
|                           | Face width                    | 136.0            | 8.9                 |                                |                            |                |   |                      |      |
|                           | Mandibular width              | 119.8            | 7.6                 |                                |                            |                |   |                      |      |
|                           | Mandibular arc                | 188.2            | 14.8                |                                |                            |                |   |                      |      |
|                           | <b>Lateral Cephalometrics</b> | Condylion-gonion | 62.5                | 7.5                            | Anterior lower face height | 58.8           | 2.9   | Gonial angle (upper) | 50.3 |
| Articulare-gonion         |                               | 44.5             | 6.5                 | Jarabak ratio                  | 82.5                       | 6.6            | Gonial angle (lower)                          | 67.8                 | 3.0  |
| Gonion-menton             |                               | 73.1             | 4.2                 |                                |                            |                | Gonial angle                                  | 118.2                | 6.9  |
| Nasion-gnathion           |                               | 105.5            | 4.4                 |                                |                            |                | Overbite Depth Indicator (ODI) <sup>165</sup> | 71.5                 | 8.3  |
| Ricketts R3-R4            |                               | 47.3             | 6.3                 |                                |                            |                |   |                      |      |
| Masseter length (caliper) |                               | 56.6             | 6.2                 |                                |                            |                |   |                      |      |

**Table 8.2** Descriptive statistics providing means and standard deviation for the 3D images and cephalometric linear, proportional and angular variables.

|    | LC             | US                 | 3D                           | Pearson Correlations r | Significance P |
|----|----------------|--------------------|------------------------------|------------------------|----------------|
| 1  | Co-Go to R3-R4 |                    |                              | 0.92                   | 0.000***       |
| 2  | Go-Me to R3-R4 |                    |                              | 0.77                   | 0.01**         |
| 3  | N_Gn to ODI    |                    |                              | -0.12                  | 0.75           |
| 4  | ODI            | Volume             |                              | 0.14                   | 0.71           |
| 5  |                | Volume - length    |                              | 0.86                   | 0.001***       |
| 6  |                | Volume - Thickness |                              | 0.95                   | 0.000***       |
| 7  | R3-R4          | Area               |                              | 0.82                   | 0.003**        |
| 8  | R3-R4          | Volume             |                              | 0.73                   | 0.01**         |
| 9  | Go-Me          | Volume             |                              | 0.66                   | 0.03*          |
| 10 | Co-Go          | Area               |                              | 0.81                   | 0.01**         |
| 11 | Co-Go          | Volume             |                              | 0.81                   | 0.01**         |
| 12 | Ar-Go          | Length             |                              | 0.72                   | 0.02*          |
| 13 | Ar-Go          | Area               |                              | 0.85                   | 0.002**        |
| 14 |                | Area               | Jaw Index                    | 0.67                   | 0.04*          |
| 15 |                | Volume             | Jaw Index                    | 0.67                   | 0.03*          |
| 16 | Go-Me          |                    | Facial Width                 | 0.83                   | 0.003**        |
| 17 | Go Angle Upper |                    | Face Height                  | 0.75                   | 0.01**         |
| 18 | Ar-Go          |                    | Mandibular Depth Linear      | 0.67                   | 0.04*          |
| 19 | Ar-Go          |                    | Mandibular Depth Curvilinear | 0.75                   | 0.01**         |
| 20 | Co-Go          |                    | t-go                         | 0.76                   | 0.01**         |
| 21 | Go Angle Upper |                    | Mandibular Inclination       | 0.70                   | 0.02*          |
| 22 | Co-Go          |                    | Facial Index Facial Ht       | 0.64                   | 0.05*          |
| 23 | Ar-Go          |                    | Jaw Index Facial Ht          | 0.73                   | 0.01**         |
| 24 | Co-Go          |                    | Jaw Index                    | 0.66                   | 0.04*          |
| 25 | Ar-Go          |                    | Jaw Index                    | 0.86                   | 0.001***       |
| 26 | ODI            |                    | Jaw Index                    | -0.11                  | 0.79           |

**Table 8.3** Pearson Correlations coefficient showing significance between the three modalities of investigation – 3D imaging, lateral cephalograms and ultrasonography. Significance is shown with (\* =  $p \leq 0.05$ , \*\* =  $p \leq 0.01$ , \*\*\* =  $p \leq 0.001$ ).

| Pearson Correlation Coefficients |       |        |            |       |        |        | (n = 10) |
|----------------------------------|-------|--------|------------|-------|--------|--------|----------|
| Linear Variables                 |       |        |            |       |        |        |          |
|                                  | N_Gn  | R3_R4  | Masseter   | Go_Me | Co_Go  | Ar_Go  |          |
| Face Height                      | 0.57  | 0.54   | 0.94       | 0.39  | 0.52   | 0.60   |          |
|                                  | 0.08  | 0.10   | <0.0001*** | 0.26  | 0.11   | 0.06   |          |
| Mandibular Height                | 0.25  | 0.33   | 0.72       | 0.16  | 0.54   | 0.66   |          |
|                                  | 0.47  | 0.35   | 0.01**     | 0.63  | 0.10   | 0.03*  |          |
| Mandibular Depth Linear          | 0.60  | 0.52   | 0.71       | 0.40  | 0.61   | 0.75   |          |
|                                  | 0.06  | 0.11   | 0.02*      | 0.24  | 0.05*  | 0.01** |          |
| Mandibular Depth                 | 0.59  | 0.51   | 0.67       | 0.42  | 0.61   | 0.72   |          |
| Curvilinear                      | 0.06  | 0.12   | 0.03*      | 0.21  | 0.05*  | 0.01** |          |
| Maxillary Arc                    | 0.39  | 0.51   | 0.48       | 0.24  | 0.55   | 0.76   |          |
|                                  | 0.25  | 0.12   | 0.15       | 0.49  | 0.09   | 0.01** |          |
| t_go                             | 0.43  | 0.57   | 0.40       | 0.57  | 0.76   | 0.62   |          |
|                                  | 0.20  | 0.08   | 0.24       | 0.08  | 0.01** | 0.05*  |          |
| go_gn                            | 0.62  | 0.39   | 0.76       | 0.46  | 0.46   | 0.59   |          |
|                                  | 0.05* | 0.25   | 0.01**     | 0.18  | 0.17   | 0.07   |          |
| Face width                       | 0.40  | -0.003 | 0.20       | 0.11  | 0.16   | 0.22   |          |
|                                  | 0.24  | 0.99   | 0.57       | 0.74  | 0.64   | 0.53   |          |
| Mandible width                   | 0.52  | 0.34   | 0.77       | 0.49  | 0.50   | 0.51   |          |
|                                  | 0.12  | 0.33   | 0.01**     | 0.14  | 0.13   | 0.12   |          |
| Mandibular arc                   | 0.59  | 0.52   | 0.65       | 0.41  | 0.61   | 0.74   |          |
|                                  | 0.06  | 0.11   | 0.04*      | 0.23  | 0.05*  | 0.01** |          |

**Table 8.4 (a)** Linear variables with Pearson correlations between 3D images and lateral cephalograms. Significance is shown with (\* =  $p \leq 0.05$ , \*\* =  $p \leq 0.01$ , \*\*\* =  $p \leq 0.001$ ).

| <b>Pearson Correlation Coefficients</b>  |                 |                      |                |            |
|--|-----------------|----------------------|----------------|------------|
| <b>Angular Variables</b>                 |                 |                      |                |            |
|  | <b>GoAngleU</b> | <b>GoAngleL</b>      | <b>GoAngle</b> | <b>ODI</b> |
| <b>Man</b>                               | -0.70           | -0.27                | -0.69          | -0.36      |
| <b>Incli-<br/>nation</b>                 | 0.02*           | 0.43                 | 0.02*          | 0.32       |
| <b>Pearson Correlation Coefficients,</b> |                 |                      |                |            |
| <b>Proportional Variables</b>            |                 |                      |                |            |
|  | <b>AFH</b>      | <b>Jarabak Ratio</b> |                |            |
| <b>IndexLJ_FH</b>                        | 0.09            | 0.32                 |                |            |
|  | 0.78            | 0.35                 |                |            |
| <b>IndexJ_FH</b>                         | 0.18            | 0.37                 |                |            |
|  | 0.61            | 0.29                 |                |            |
| <b>Facial index</b>                      | 0.75            | -0.42                |                |            |
|  | 0.01**          | 0.22                 |                |            |
| <b>Jaw index</b>                         | 0.26            | 0.28                 |                |            |
|  | 0.45            | 0.43                 |                |            |
| <b>Index jaw facial width</b>            | 0.65            | -0.33                |                |            |
|  | 0.04*           | 0.34                 |                |            |
| <b>Index jaw width facial<br/>height</b> | 0.09            | 0.32                 |                |            |
|  | 0.78            | 0.35                 |                |            |

**Table 8.4 (b)** Angular and proportional variables with Pearson correlations between 3D images and lateral cephalograms (\* =  $p \leq 0.05$  significant) and (\*\*=  $p \leq 0.01$  highly significant) values.



| <i>3D Variables &amp; Indices</i> | <i>SD</i> | <i>SE</i> | <i>Dahlberg<br/>Statistic</i> |
|-----------------------------------|-----------|-----------|-------------------------------|
| Face Width                        | 9.54      | 3.01      | 8.86                          |
| Mandible Width                    | 4.64      | 1.47      | 0.92†                         |
| Face Height                       | 4.26      | 1.35      | 0.44††                        |
| Mandible Height                   | 4.93      | 1.56      | 3.93                          |
| Maxilla Arc                       | 12.75     | 4.03      | 21.52                         |
| Mandibular Depth Linear           | 5.79      | 1.83      | 8.66                          |
| Mandibular Depth Curvilinear      | 6.98      | 2.21      | 12.06                         |
| Mandibular Arc                    | 13.97     | 4.42      | 24.11                         |
| Mandibular Inclination            | 6.93      | 2.19      | 12.52                         |
| Facial Index                      | 14.95     | 4.73      | 5.52                          |
| Jaw Index                         | 4.22      | 1.34      | 0.70†                         |
| Index Jaw/Facial Width            | 13.77     | 4.36      | 9.03                          |
| Index Jaw Width/Facial Height     | 6.84      | 2.16      | 2.97                          |
| Index Lower Jaw/Facial Height     | 1.99      | 0.63      | 3.17                          |
| Index of Jaw/Facial Height        | 9.75      | 3.08      | 5.11                          |
| t-go                              | 6.31      | 2.10      | 7.90                          |
| go-gn                             | 5.42      | 1.72      | 7.59                          |

**Table 8.5** Error method for 3D variables in linear and index measurements. †† show very low error and † moderately low error, hence the significance of these measurements with enhanced repeatability (Dahlberg's Statistics).

| 3D landmarks | Mean       | Standard  | Standard | Sum of errors | Dahlberg |
|--------------|------------|-----------|----------|---------------|----------|
|              | Difference | Deviation | Error    |               |          |
| Nasion x     | -0.07      | 0.09      | 0.03     | -0.68         | 0.15     |
| Nasion y     | -0.02      | 0.04      | 0.01     | -0.20         | 0.05     |
| Nasion z     | -0.02      | 0.03      | 0.01     | -0.20         | 0.05     |
| Sub Nasale x | -0.06      | 0.12      | 0.04     | -0.62         | 0.14     |
| Sub Nasale y | 0.00       | 0.05      | 0.02     | -0.04         | 0.01     |
| Sub Nasale z | 0.02       | 0.07      | 0.02     | 0.16          | 0.04     |
| glabella x   | -0.03      | 0.08      | 0.02     | -0.30         | 0.08     |
| glabella y   | 0.02       | 0.04      | 0.01     | 0.17          | 0.04     |
| glabella z   | 0.00       | 0.02      | 0.01     | 0.02          | 0.01     |
| gnathion x   | -0.02      | 0.07      | 0.02     | -0.22         | 0.05     |
| gnathion y   | -0.02      | 0.08      | 0.03     | -0.21         | 0.05     |
| gnathion z   | 0.02       | 0.07      | 0.02     | 0.21          | 0.05     |
| go-right x   | 0.06       | 0.18      | 0.06     | 0.64          | 0.14     |
| go-right y   | 0.01       | 0.11      | 0.03     | 0.15          | 0.03     |
| go-right z   | -0.02      | 0.14      | 0.05     | -0.20         | 0.04     |
| pogonion x   | -0.42      | 1.64      | 0.52     | -4.24         | 0.95     |
| pogonion y   | 0.01       | 0.26      | 0.08     | 0.13          | 0.03     |
| pogonion z   | -0.26      | 0.75      | 0.24     | -2.63         | 0.59     |
| stomion x    | -0.02      | 0.14      | 0.05     | -0.22         | 0.05     |
| stomion y    | 0.00       | 0.04      | 0.01     | -0.04         | 0.01     |
| stomion z    | 0.00       | 0.05      | 0.02     | 0.05          | 0.01     |
| tragus x     | -0.06      | 0.26      | 0.08     | -0.65         | 0.15     |
| tragus y     | -0.05      | 0.08      | 0.02     | -0.55         | 0.12     |
| tragus z     | 0.18       | 0.23      | 0.07     | 1.81          | 0.41     |
| zy x         | 0.22       | 0.19      | 0.06     | 2.17          | 0.48     |
| zy y         | 0.00       | 0.04      | 0.01     | 0.02          | 0.00     |
| zy z         | 0.10       | 0.22      | 0.07     | 1.01          | 0.23     |

**Table 8.6** Reproducibility of the 3D coordinates x,y,z assessed with Dahlberg's statistics.

| Pearson Correlation Coefficients |                    |                  |                     |                     |                    |
|----------------------------------|--------------------|------------------|---------------------|---------------------|--------------------|
| (n=10)                           |                    |                  |                     |                     |                    |
|                                  | Linear3D_<br>Fact1 | Prop3D_<br>Fact1 | Linear3Dw_<br>Fact1 | Linear3Dw_<br>Fact2 | Man<br>Inclination |
| <b>US-Fact1</b>                  | 0.43*              | 0.37             | -0.06               | -0.37               | -0.02              |
|                                  | 0.22               | 0.30             | 0.87                | 0.30                | 0.96               |
| <b>US-Fact2</b>                  | 0.64**             | 0.27             | 0.11                | -0.40               | -0.03              |
|                                  | 0.05               | 0.45             | 0.75                | 0.26                | 0.93               |
| <b>Linceph-Fact1</b>             | 0.72**             | 0.32             | -0.04               | -0.35               | 0.04               |
|                                  | 0.02               | 0.37             | 0.91                | 0.32                | 0.92               |
| <b>Angceph-Fact1</b>             | 0.05               | 0.15             | -0.26               | -0.17               | -0.65**            |
|                                  | 0.89               | 0.70             | 0.49                | 0.67                | 0.06               |
| <b>Angceph-Fact2</b>             | -0.33              | -0.54*           | 0.32                | -0.35               | 0.06               |
|                                  | 0.39               | 0.13             | 0.41                | 0.36                | 0.87               |
| <b>Prpceph-Fact1</b>             | -0.21              | -0.14            | -0.25               | -0.29               | 0.08               |
|                                  | 0.57               | 0.70             | 0.49                | 0.42                | 0.84               |
| <b>Linear3D-Fact1</b>            | 1.00               | 0.59             | 0.29                | -0.28               | -0.32              |
|                                  |                    | 0.07             | 0.42                | 0.44                | 0.37               |
| <b>Prop3D-Fact1</b>              | 0.59               | 1.00             | 0.26                | 0.00                | -0.18              |
|                                  |                    |                  | 0.07                | 0.99                | 0.61               |
| <b>Linear3Dw-</b>                |                    |                  |                     |                     |                    |
| <b>Fact1</b>                     | 0.29               | 0.26             | 1.00                | -0.17               | 0.09               |
|                                  | 0.42               | 0.46             |                     | 0.63                | 0.81               |
| <b>linear3Dw-</b>                |                    |                  |                     |                     |                    |
| <b>Fact2</b>                     | -0.28              | 0.00             | -0.17               | 1.00                | 0.62**             |
|                                  | 0.44               | 0.99             | 0.63                |                     | 0.05               |
| <b>Man Inclination</b>           | -0.32              | -0.18            | 0.09                | 0.62**              | 1.00               |
|                                  | 0.37               | 0.61             | 0.81                | 0.05                |                    |

**Table 8.7** Factor analyses and Pearson correlations among the 3D images, lateral cephalograms and US. Factors 1 constitutes thickness and volume of masseter muscle while Factor 2 is length and area of masseter muscle. \* =p < 0.05, \*\*=p < 0.01.

Predictive equations were developed from multiple linear regression analyses and were chosen as significant (Table 8.8) on the basis of higher proportional to the variance. The  $\beta$ -weights were added into the equations. However, only a few variables qualified for predictive equations to be significant such as tragus to gonion, mandibular arc, mandibular depth curvilinear/linear, and face heights.

## 8.5 DISCUSSION

It's aptly stated that beauty lies in the eyes of the beholder; however, Farkas variables try to quantify attractiveness<sup>154</sup> and provide scientific evidence. Others have considered the application of the divine proportion, more for the dental tissue display and attractiveness<sup>220, 221</sup>. Thus, previous work has attempted to use numbers to define attractiveness.

Landmarks provided by anthropometry have served well over many decades and can be conveniently translated into 3D imaging. However, certain factors need to be accounted for in order to produce a high level of accuracy. The examiner's skill and ability to identify features are of paramount importance followed by the quality and resolution of the images, unlike real-time anthropometry where cooperation and stillness of the live subject are critical<sup>153</sup>. Moreover, correct head orientation is necessary to standardize measurements among and between patients<sup>222</sup>. Commonly, Frankfurt Horizontal is taken as a reference plane but recent work<sup>223, 224</sup> suggests the Krogman-Walker (KW) line is equally effective and practical for estimating head orientation. Alternatively, sophistication of measuring tools and the e-tools in software could prove a valuable addition to 3D morphometry providing a wider scope and accuracy not possible with conventional anthropometry. Interestingly the indices with larger measurements had poorer reproducibility as compared to more compact and close measurement relationships.

| Predictive Equation  | R <sup>2</sup> | MSE  | SIG |
|--|----------------|------|-----|
| <b>Linear Variables</b>  |                |      |     |
| R3-R4 = 25.44932 + 0.48688*t-go  | 0.33           | 5.46 | *   |
| Masseter = -37.9501 + 0.81574*FaceHt                                     | 0.88           | 2.19 | *   |
| N-Gn = 75.76050 + 0.20701*go-gn + 0.10290*ManDepthLinear                 | 0.42           | 3.83 | *   |
| Masseter = -45.1784 + 0.67128*FaceHt + 0.20006*Mandiblewidth             | 0.92           | 1.98 | *   |
| Go-Me = 58.13533 + 0.06039*Mandibulararc                                 | 0.17           | 4.06 |     |
| Co-Go = 28.11536 + 0.76730*t-go  | 0.58           | 5.14 | *   |
| Ar-Go = -8.69762 + 2.50677*ManDepthLinear + -1.93239*ManDepthCurvilinear | 0.67           | 4.16 | *   |
| <b>Angular Variables</b>   |                |      |     |
| GoangleU = 71.06816 + -0.36734*ManIncli                                  | 0.49           | 4.13 |     |
| Goangle = 144.2894 + -0.46133*ManIncli                                   | 0.47           | 5.33 |     |
| <b>Proportional Variables</b>  |                |      |     |
| AFH = 52.67724 + 0.11825*Indexjawwidthfacialheight                       | 0.01           | 3.06 |     |
| AFH = 52.71398 + 0.18845*JawIndex  | 0.07           | 2.96 |     |
| AFH = 54.06144 + -0.03102*Indexjawwidthfacialheight + 0.19646*JawIndex   | 0.07           | 3.17 |     |
| JarabakR = 109.0283 + -0.20828*Indexjawfacialwidth                       | 0.11           | 6.62 |     |
| JarabakR = 69.87241 + 0.24662*IndexJaw-FH                                | 0.13           | 6.52 |     |
| JarabakR = 101.1132 + -0.27080*Indexjawfacialwidth + 0.30918*IndexJaw-FH | 0.32           | 6.2  |     |

**Table 8.8.** Predictive Tables for the various 3D imaging variables that can provide information pertaining to lateral cephalometric variables. Starred equations show significance at the level of  $p < 0.05$ . Linear measurements have the statistically significant predictive equations. Gray bars are the  $\beta$ -weights.

We used simple methods to produce prediction equations rather than the more resource intensive Bayesian or Monte Carlo factor models with the aim of, decreasing the complexity and making it more clinically applicable. The concept of generating predictive equations from 3D images for lateral cephalometric variable estimation has been presented for the first time. Although, it can be debated that with a small sample size the value of such prediction is questionable, it does set the scene for future work.

Compared to the reported Eigenvalues from Benington *et al*<sup>200</sup> our values were lower. Also their study was the first to document the masseter volume measurements with high technology 3D US scanning. Likewise, the current study did measure masseter volume, albeit indirectly, utilizing a simple, portable US unit that could find application in clinical settings. Similarly, when compared with Radsheer<sup>204</sup>, our values were slightly lower but their study included, 121 adults and previous work with 329 subjects aged 7-22 from a Greek population<sup>127</sup>. Our result differences could be attributed to the sample size and also the population from which they are selected.

The method error indicated that there were certain landmarks that had reduced repeatability. This may be explained by background noise and lack of clear definition in some scans. Palpation is generally advantageous in precise positioning of soft tissue gonion, but it is considered a difficult point overall to determine even in anthropology<sup>126</sup>. Nasion (n) and subnasale (sn) were relatively easily identified on the 3D images. For a better view, the image was rotated upwards by 30°. This is an advantage of the scans because repositioning the live patient can be difficult and sometimes embarrassing. The accuracy and repeatability of 3D Imaging has been documented as exceptional<sup>225</sup> and, as with most recordings, in order to eliminate inter-operator variability all measurements should be made by the same investigator. The angular measurements are dependent on head position and need to be standardized across the sample<sup>126</sup>.

The curvilinear measurements were included because they are more biologically meaningful than straight line representations of complex 3D structures (Fig 8.4). For example, our findings show a significant difference ( $p < 0.0001$ ) at 95% CI and with a standard error of 0.52 and SD = +/- 1.65 for the linear mandibular depth compared to

the curvilinear mandibular depth. The mandibular curvilinear arc extended from left tragus to subnasale to right tragus (t-sn-t) and did not have an equivalent linear counterpart. The use of curvilinear measures is gaining application in tooth morphology studies where curvilinear measurements are deemed superior to the conventional linear ones<sup>226, 227</sup>.

### 8.5.1 MUSCLES OF MASTICATION

Muscle volume and cross section is important in the diagnosis of facial dysmorphia<sup>228</sup> and 3D imaging is invaluable for long-term soft tissue changes, especially in hemifacial microsomia<sup>229</sup>. US is making its way into diagnostics and although we had moderate correlations with lateral cephalometrics and 3D imaging there is future scope with technological advances in US. Overall, 3D imaging is widely used to evaluate growth changes<sup>146, 147</sup> and evaluate treatment effects particularly with functional orthopaedic appliances.

Previous work has used MRI for comparing masseter muscle with cephalometric variables<sup>104, 156</sup>, but accepting that MRI is expensive and difficult for routine patient evaluation, our study endeavoured to explore more cost-effective ways of imaging the masseter muscle.

### 8.5.2 SCOPE AND APPLICATION OF IMAGING

Baumrind eloquently stated that the “craniofacial complex system needs to be evaluated from different perspectives as no single view would do justice in its evaluation and future treatment planning”<sup>230</sup>. 3D imaging has extended not only to facial surface analyses but is extending to cephalometry as well<sup>222</sup>. Subtle soft tissue changes have been studied extensively in recent work particularly with pre- and post-treatment outcomes<sup>109, 134, 149, 231-234</sup>. Similar interest with mandibular growth changes<sup>231</sup> and four-dimensional analyses for the TMD<sup>234</sup> are gaining momentum in diagnostic imaging. A common critique with new imaging techniques has been the reliability which is of concern and can be addressed with the development of self – calibrating measuring systems<sup>134</sup>.

New directions in technology will soon be evident with the need to enhance the quality of 3D images with more real-life effect. This would assist in patient education and teaching sessions for dental students. Moreover, programs with substantial mouse manipulation create undue hand and wrist fatigue whereas touch screen options would be ergonomically valuable.

Clinical applications of 3D imaging are vast and numerous. From treatment planning to pre- and post-treatment evaluation, the images can be manipulated from any direction providing in-depth analysis of the case without patient recalls and inconvenience of anthropometry. It is becoming a vital tool in orthognathic surgery planning, patient education, “*tele-orthodontics*”<sup>108</sup> to manage global movement of patients, and where interdisciplinary treatments are sought. It is an effective recording method for various facial asymmetries<sup>225</sup> and severe craniofacial dysostoses, hemifacial microsomias<sup>228</sup>, and where simple photographs have serious limitations. The non-invasive nature of 3-D imaging will make its application widely accepted for sequential evaluation in growing children and on controls for research

225

However, the idea of obviating lateral cephalograms entirely may not yet be the case because radiographs still provide valuable skeletal and dental information vital for initial treatment planning. Moreover, we do acknowledge the limitations of prediction because as with any prognostic approach, particularly in a biological system, there will be variations. However, a method that can assist the clinician in reducing the number of radiographic investigations would surely be welcomed by the public and profession alike.



## 8.6 CONCLUSIONS

- 1) Statistically significant correlations were observed between lateral cephalometric variables and 3D images.
- 2) US and 3D images had moderate correlations with area and volume of the masseter muscle which were used to generate predictive equations.
- 3) The reproducibility and method error were within acceptable range but could be improved with better software designs.
- 4) 3D images need to be of high quality, preferably with natural colours, to simulate the reality needed for use in clinics and patient education.
- 5) The images captured should be easy to manipulate preferably with touch screen options thus creating more ease and efficiency.
- 6) A larger sample size accounting for racial differences would be required to generate more meaningful predictive equations.
- 7) Curvilinear measurements are more biologically meaningful than simple, straight line representations.

### 8.6.1 ACKNOWLEDGEMENTS

We appreciate the funding provided by the Australian Dental Research Foundation and Dr J Fricker, Tidbinbilla Canberra, ACT Australia and Dr.S Vallance, senior research officer, Mona Lisa Imaging (scott@monalisaimaging.net). Our sincere thanks go to the staff at UniSA for their collaboration with the project, Dr Nancy Briggs (The University of Adelaide) for statistical analyses and Mrs Lucy Hatch for secretarial assistance.

## 9 SUMMARY AND CONCLUSIONS

In orthodontics there is a strong association between form and function<sup>235</sup>. This has been studied extensively and proved with strong correlation that exists between the soft tissue and underlying osseous foundation. However, there are not many studies from the muscles perspective, particularly, the muscles of mastication including the masseter. The work presented in this thesis supports the results from previous reports; especially, the masseter muscle dimensions and its correlations to vertical facial proportions (Chapter 6,7,8). This project further elucidated dynamic function from spindle responses with EMG recordings (Chapter 5) in different facial proportion which hasn't been done previously. Hence, the inability to compare our data with previous published research.

Facial form was further investigated with ultrasonography for different dimensions of masseter muscle and correlations of measurements with lateral cephalometric and 3D images. For the first time simple predictive equations were generated to provide alternative means of deducing information from single rather than multiple investigations (Chapter 7,8) and may offer future research opportunities to minimize ionizing radiation.

### 9.1 MASSETER MUSCLE SPINDLES

The present EMG study is the first to incorporate a dynamic component and showed a masseter muscle spindle response that correlated with vertical facial dimensions derived from the lateral cephalograms (Chapter5). There is no previous work with which to compare these findings.

The masseter muscle is densely populated with spindles and hence became the choice for this project. The spindles showed high excitation during the opening phase and is contrary to what would otherwise be expected. Suggestions have been put forward to use H-reflex methodology rather than mechanical stimulation for excitation of muscle spindles as this would further limit noise in the data recordings (Chapter 4).

From a physiological perspective, this information provides new direction to explore dysfunctions and muscle spindle response in conditions that currently lack therapeutic interventions.

EMG recordings are only good if strict standardization is followed in the protocol as noise can produce erroneous results. Moreover, EMG recordings cannot be simply translated into other variables such as force generation, muscle length and synergy among muscles as the relationship is complex and entails interplay of several other factors.

Muscle spindle reflexes do contribute to force generations by fine tuning and this has been verified in several studies<sup>3, 236, 237</sup>. It is evident by the substantial drop of force capacity in patients who are rendered edentulous and attempt learning to chew with a removable prosthesis. One study found 20-40% loss in the masticatory force<sup>238</sup> and reinforced the significance of PMR and other peripheral inputs to muscle spindles.

EMG has previously been used to evaluate stability in post-orthodontic cases<sup>239</sup> and more recently, Mechanomyograms and EMG combinations have been used by *loi et al.*<sup>240</sup> to investigate masseter muscle fatigue.

## 9.2 MASSETER MUSCLE DIMENSIONS

Masseter muscles can be accurately measured by US and other imaging techniques such as CT and MRI. However, the project aimed to find methods that were non-invasive, cost-effective and could easily be translated into clinical settings.

The factor analyses conducted with US, lateral cephalograms and 3D imaging enabled comparisons with previous work which used similar parameters<sup>200, 204</sup>.

Furthermore, for this project a simple measurement off the lateral cephalogram using bony landmarks to identify the origins and insertions of the superficial masseter (Chapter 7 and 8) were taken. Correlations with the US measurements were then generated but showed moderate correlations only with  $r=0.58$  ( $p=0.06$ ). This would certainly not be clinically acceptable.

The masseter muscle is a skeletal muscle which, as any other, has the potential for hypertrophy and hyperplasia<sup>241</sup>. Lengthening of the muscle results in the addition of sarcomeres which contributes to an overall increase in muscle mass. Interestingly, this potential is higher during growth as compared to mature muscle cells which have limited ability to divide. Perhaps this contributes to the success rate observed with functional orthopaedic appliances but evidence is currently lacking. Goto *et al.*<sup>21</sup> used optical jaw tracking with MRI to assess the fibre length changes during jaw movements. With the complex multipennate structure it is not surprising that the masseter fibre lengths contract and lengthen differentially along the length of the entire muscle. Goto found the largest increase in muscle length in the medial part of the deep masseter (34-83%) while the smallest change appeared in the posterior most superficial masseter and ranged from between 2-19%. One could conclude from such findings that the complexity of the muscle demands very detailed investigation. Furthermore, one could speculate that it accounts for some of the variation we observe with the success of functional orthopaedic appliances. There has always been anecdotal evidence tendered to explain functional orthopaedic appliance success, but different individuals would most likely have differing muscle physiology and even changes in ramp or bite height of an appliance could make the difference between success and failure.

Masseter muscle volume has importance and has been the focus of recent studies.<sup>122, 130, 200</sup>. Masseter muscle volume differences are profound in patients with hemifacial microsomia<sup>229</sup>. CT scans were utilized in that study but our method with US provides a safer and more cost-effective alternative.

Both conventional and 3D ultrasound have been used in orthodontics and several papers have found high correlations between vertical face heights with thickness and volume of masseter muscle<sup>130, 200</sup>. We selected the midpoint of muscle thickness for our study as its advocated for the highest reproducibility<sup>242</sup>.

The predictive values generated from the correlations were not very strong, rather lengthy and difficult to apply with confidence. Hence, current findings do not support the use of US and lateral cephalometric predictive equations (Chapter 7) due to dimensional variations of the measurements<sup>21</sup>.

There is definitely scope for US for assessment of masseter muscle in real-time. This has been documented widely in the literature with masseter muscle thickness demonstrating differences in posterior crossbite cases and their relationship to TMDs<sup>106, 125, 212, 213</sup>. But there is concern that some findings can be controversial and others produce non-conclusive results. For example, some studies<sup>23</sup> found the crossbite side had thinner masseter muscle. Obviously, 3D US is superior in function and would be better for oro-facial applications<sup>200</sup> provided it is cost-effective. One can also anticipate the rapid advancement in technology and 4D US may well be the future for diagnosis and treatment evaluation.

### 9.3 3D IMAGES

3D imaging was used for the superficial soft tissue measurements and transverse indices. Once again the findings were similar to past work. Currently, the imaging is still a single capture in time and presents limited insight into the true functional assessment. Even though there are several existing packages available for 3D imaging it has yet to become a routine diagnostic tool. There are several reasons for not having 3D imaging in mainstream clinical set ups. Primarily the cost, followed by *not completely realistic* imaging which still needs refinement for accurate and life-like reproduction of the face. Also, the data acquired from such analyses needs to be unique and provide information that cannot be generated by other more conventional means. Finally, the product needs to be user-friendly and easy to apply by the clinician or auxiliary staff. Above all, the suggestion that 3D imaging could be a surrogate for lateral cephalograms with predictive correlations obviating the need for serial radiography and radiation exposure, could make it an attractive choice.

The current study has found high correlation of certain lateral cephalometric variables, particularly the vertical ones, with 3D imaging indices (Chapter 8 Results). However, before it enters into mainstream clinical practice, the following criteria need to be fulfilled.

**Reliability** is considered a composite of repeatability and reproducibility<sup>160</sup> and different 3D imaging techniques have been scrutinized for accuracy and reliability. Kusnoto and Evans<sup>243</sup> used a surface laser scanner ( Minolta Vivid 700) to assess

various objects ranging from cylinders to cast analyses and facial models. They found accuracy in the range of 1.9 +/- 0.8mm for facial imaging which was not as high as for cast analyses 0.2 +/- 0.2mm. Hence one can conclude that the larger the surface to scan and the greater the data acquisition, the higher the error rate with current 3D scans. Likewise, the suggestions for improvement and exploring more user-friendly options in 3D technology have been highlighted in a review article addressing these issues<sup>233</sup>.

**Standardization** is equally essential for the translation of the predictive equations across the board with different imaging packages. This has been norm with many software cephalometric packages currently in use and could become an overall package.

**Cost Effectiveness** and ease of accessibility with perhaps even free downloads such as used in this study (Chapter 8) can enhance its wider applicability. Such off-line computer analyses can provide flexibility and effective access<sup>244</sup>. However, one has to be wary of the quality of such softwares; reproducibility, reliability, accuracy of reproduction and ease of manipulation. Perhaps custom-made software packages specifically tailored to orthodontic case assessment<sup>226, 227</sup> with higher resolution and reproducibility would be welcomed by the profession. Overall such endeavour will aid in patient education and serve as a vital teaching tool to students to appreciate subtle changes during treatment and growth.

### **Safety**

Efforts are being made to assess mandibular growth with 3D MRI<sup>231</sup>. However, there is real concern about the justification of such expensive investigations and is often under fire for overuse in certain countries. Clearly, for the conventional orthodontic patient such scans would not be routinely recommended.

Multiple investigations used in the past such as CT, MRI and radiographs can be replaced with carefully selected diagnostic and evaluating tools which provide maximum information with minimal hazard along with the added bonus of being cost-effective. The current work has addressed this issue and future investigations should be geared to validate it.

## 9.4 METHOD ERROR

The method error for this research was evaluated with Dahlberg's statistic (DS) which is commonly recommended in dental research<sup>206</sup>. Bland and Altman were constructed for US and 3D x,y,z co-ordinates<sup>167</sup>.

The hypothesis of masseter muscle evaluation using a simple caliper method on standard lateral cephalograms had to be rejected on the grounds of poor Pearson correlation coefficients between the caliper readings and the actual length determined with US ( $r=0.58$ ;  $p=0.06$ ). This study does not recommend simple alternative methods for masseter muscle assessment because measurements off a US screen produce greater accuracy.

Recent work has explored the correlations between anthropometric and cephalometric measurements of vertical profile<sup>209</sup>. The study found nasion and menton to be highly correlated between the two investigation, but landmarks such as subnasale, supradentale and infradentale varied significantly. This could be due to the overlying soft tissue and its variability among individuals. For this particular reason we chose landmarks that would be more closely related to the cephalometric counterparts such as glabella, nasion, gnathion, subnasale, gonion, zygion, orbitale, tragus and stomion.

However, due to difficulties in lateral projections inherent to the Structured Light (SL) technique we consistently had difficulty in locating the tragus. Overall, our best and most highly repeatable landmarks were soft tissue subnasale (y-axis) with Dahlberg's statistic (DS) = 0.009, followed by zygion (y-axis) DS=0.004, glabella (z-axis) with DS=0.005 and stomion (z-axis) DS=0.01. The above mentioned landmarks provide a reliable array of reference points to include in future 3D assessments. However, the majority of the 3D landmarks were within an acceptable range. Details of the 3D results are provided in Chapter 8. Perhaps the repeatability could be enhanced with refined software with greater matrix size and pixel ratio<sup>160</sup>. This would further refine the accuracy of the prediction equations and improve overall reliability.

Currently, work is in progress in Liverpool where Brook *et al.* are evaluating 3D imaging for better assessment of surface contours of teeth<sup>226, 227, 245</sup>. Precision and accuracy with e-tools will improve the way we measure. Thus, more studies will be needed to explore landmark assessment and measurement

## 9.5 PREDICTIVE EQUATIONS

The present work, has for the first time looked into the possibility of a simple mathematical model enabling the interchangeable use of different investigating tools. There are some strong correlations between the data sets from US and 3D imaging (Chapter 8) and the predictive equations generated from those appear promising. Understandably, these two tools are measuring similar but not identical landmarks and region. However, more in-depth work would be required prior to accepting this model. Such equations are now possible with multiple regression analyses and recent work by Kneafsey *et al.*<sup>160</sup> suggests that such mathematical models are valid. One of the major criticisms of prediction, particularly for soft tissues, is the high individual variability. To compound the issue further, the prediction equation is as good as the initial reproducibility of the imaging set for the task; hence, pattern recognition and ability to generate curvilinear ratios are important.

Statistical packages with robust systems to produce prediction equations can be utilized for improved equations. Some recommended methods are the Bayesian approach or for prediction tables with the Monte Carlo method<sup>206</sup>. One needs to be mindful that such statistical analyses can be resource intensive.



## 9.6 CLINICAL APPLICATIONS

The oro-facial region is a highly complex system and cannot be analysed by just one mode of assessment. It needs 3D assessment with accuracy and reproducibility. Of the available options in 3D imaging<sup>110</sup> which include photogrammetry, lasers, video imaging, MRI, CT, US and structured light technique, the last two seem to be the least invasive and most cost-effective. To this endeavour, different technological advancements in the future will provide the finesse that orthodontic case assessment requires. Moreover, the possibility for research and insight into aetiology could be endless. The clinical implications of these non-invasive imaging tools can be phenomenal; apart from routine diagnosis, progress and development, it is implied that 3D imaging along with US will be available for Forensic sciences, predictions, genetics and family data<sup>139</sup>. Our current understanding is limited for the more sinister conditions which affect the masseter muscle; such as myasthenia gravis, muscular dystrophies, Duchenne's muscular dystrophy, myotonic dystrophy, myositis ossificans traumatica and Guillain-Barré syndrome<sup>9</sup>. These conditions could benefit from research using EMG and multivariate investigations to enhance our understanding of the real-time physiology of such pathologies.

## 9.7 FUTURE APPLICATIONS IN ORTHODONTICS

Interestingly, recent work has been geared towards functional assessment of the orofacial region with innovative tools. However, most of these are too costly to apply into clinical practice until the technology becomes mainstream. Until then it would be worthwhile to provide some information with alternative mathematical algorithms such as predictive equations. There has been a surge in the use of predictive tables in the last few years particularly in orthognathic surgery<sup>160</sup> and functional appliance efficacy<sup>246</sup>. Applications of predictive tables, provided they are robust and valid, can be endless particularly in research where time-consuming clinical trials are generally the norm. With rising cost for research and difficulties in ethical approval, such an approach could provide valuable information.

Work is in progress with every effort being made to reduce the radiation exposure particularly in children. In Japan, non-radiographic cephalometric systems are being explored<sup>247</sup>. Such innovation, once refined and reproducible, would provide added advantage of portability and applications in epidemiology. This could be further translated into US and 3D imaging additions.

Finally, although orthodontics is commonly associated with aesthetics and cosmetic needs of the patient, it is closely related to improving the quality of life<sup>248</sup> and the efforts made in this study were aimed toward improved investigatory methodology which would prove safe, cost-effective and user-friendly.

## 9.8 FINAL REMARKS

The aim of this research was to explore the active masseter muscle from multiple aspects. It provided insight into the role of the masseter muscle spindles and relationship to facial dimensions. The masseter was evaluated with US and 3D imaging to quantify it with minimal intervention and find correlations with facial form. Finally, information regarding the strengths of 3D curvilinear measurements and their significance for future research, along with the predictive equations for multiple analyses were investigated.

We are well aware of the implications of translating information from one investigating medium to another and amalgamating 2D and 3D data is not an easy task. In fact, there can be oversimplifications and assumptions that can add to error. One common example is that the cephalometric dimensions can be overestimated when 3D images are used, possibly due to the soft tissue presence and the 3D nature of the acquisition of data<sup>145</sup>. Large scale studies along with FEA (Finite Element Analysis) can help us understand better how to eliminate such sources of inaccuracies.

We do acknowledge the limitations of a small sample size but the results suggest that, if carried out on a large scale with due allowances for the facial classifications and ethnicity, a *group specific equation* model could be generated. Moreover, prospective trials are needed to verify the validity of appropriate predictive

equations<sup>160</sup>. Soft ware generated specifically for such use could make it more accessible and applicable.

Ideally, a diagnostic evaluation encompassing all features of soft, osseous and dental tissue in three dimensions i.e sagittal, transverse and vertical with time, the 4<sup>th</sup> Dimension<sup>231, 234</sup> would give us a more holistic approach to diagnosis, treatment planning and dento-facial evaluation in orthodontics. Future techniques will add another aspect with animated records along with projection of the fourth dimension for the course of growth and / or treatment. 3D imaging of tongue movements and position has been shown to be statistically significant in cross-bite cases<sup>214, 234</sup>.

Our understanding of malocclusion has come a long way but it is multidimensional, multifaceted and highly variable and needs to be analyzed from several different perspectives. The emphasis is shifting from static, radiation-based investigations which are a snap shot in time to dynamic real-time recordings of soft tissue function. The fourth dimension in combination with conventional diagnostic tools could provide a comprehensive single diagnostic package that would not only assist in complete records diagnosis and evaluation but provide predictions for future expected changes.